

AD-A104 303

UNITED TECHNOLOGIES RESEARCH CENTER EAST HARTFORD CT  
THEORETICAL RESEARCH INVESTIGATION UPON REACTION RATES TO THE N--ETC(U)

F/G 4/1

JAN 80 M H MICHELS

F19628-77-C-0248

NL

UNCLASSIFIED

AFGL-TR-80-0072

1 OF 1  
40 A  
A104103

END  
DATE  
FILED  
10-81  
DTIC

AFGL-TR-80 -0072

LEVEL II

(12)

AD A104303

THEORETICAL RESEARCH INVESTIGATION UPON  
REACTION RATES TO THE NITRIC OXIDE  
(POSITIVE) ION

H. Harvey Michels  
United Technologies Research Center  
East Hartford, Connecticut 06108

31 January 1980  
Final Report  
77 Sept - 79 Dec 31

DTIC  
ELECTED  
S SEP 17 1981  
E

Approved for public release; distribution unlimited

This research was supported by the Defense Nuclear Agency under Subtask S99QAXHD028, Work Unit 44, entitled "Computations of Molecular Structures and Transition Probabilities."

Air Force Geophysics Laboratory  
Air Force Systems Command  
United States Air Force  
Hanscom AFB, Massachusetts 01731

DTIC FILE COPY

819 17 025

**Qualified requestors may obtain additional copies from the  
Defense Technical Information Center. All others should  
apply to the National Technical Information Service.**

Unclassified

SECURITY CLASSIFICATION OF THIS PAGE (When Data Entered)

REPORT DOCUMENTATION PAGE			READ INSTRUCTIONS BEFORE COMPLETING FORM	
1. REPORT NUMBER AFGL-TR-80-0072	2. GOVT ACCESSION NO. AD A104303 G	3. RECIPIENT'S CATALOG NUMBER		
4. TITLE (and Subtitle) Theoretical Research Investigation Upon Reaction Rates to the Nitric Oxide (Positive) Ion.	5. TYPE OF REPORT & PERIOD COVERED Final Report CP 11-12 Dec 30 71			
6. AUTHOR(s) H. Harvey/ Michels	7. CONTRACT OR GRANT NUMBER(s) F19628-77-C-0248			
8. PERFORMING ORGANIZATION NAME AND ADDRESS United Technologies Research Center East Hartford, Connecticut 06108	10. PROGRAM ELEMENT, PROJECT, TASK AREA & WORK UNIT NUMBERS 62704H DNA 27AB			
11. CONTROLLING OFFICE NAME AND ADDRESS Air Force Geophysics Laboratory Hanscom AFB, MA 01731 Contract Monitor: Dr. Frederick R. Innes/PHG	12. REPORT DATE January 1980			
14. MONITORING AGENCY NAME & ADDRESS (if different from Controlling Office)	13. NUMBER OF PAGES 65			
15. SECURITY CLASS. (of this report) Unclassified				
15a. DECLASSIFICATION/DOWNGRADING SCHEDULE				
16. DISTRIBUTION STATEMENT (of this Report) Approved for public release; distribution unlimited.				
17. DISTRIBUTION STATEMENT (of the abstract entered in Block 20, if different from Report)				
18. SUPPLEMENTARY NOTES This research was supported by the Defense Nuclear Agency under Subtask S99QAXHD028, Work Unit 44, entitled: "Computation of Molecular Structures and Transition Probabilities."				
19. KEY WORDS (Continue on reverse side if necessary and identify by block number) NO+ electronic structure charge transfer cross section				
20. ABSTRACT (Continue on reverse side if necessary and identify by block number) Theoretical investigations of the electronic structure and radiative transition probabilities of atmospheric species and of kinetic reaction rates for electron-ion ion-atom, and ion-molecule reactions are in progress. These investigations are being carried out using quantum mechanical methods and digital computer codes which represent state-of-the-art numerical techniques. The electronic structure and static molecular properties are				

DD FORM 1 JAN 73 1473

EDITION OF 1 NOV 65 IS OBSOLETE

S N 0102-LF-014-6601

Unclassified

SECURITY CLASSIFICATION OF THIS PAGE (When Data Entered) 4042

being studied using ab initio configuration-interaction wavefunctions which have sufficient flexibility to properly connect with the ground and excited asymptotic atomic and ionic limits. The charge transfer cross-sections are computed using a semi-classical close-coupling code which has been developed in this Center. Modified Numerov integration techniques are employed to evaluate the matrix elements for the dissociative-recombination cross-sections. The branching into the reaction product channels can also be calculated using a full quantum multichannel close-coupling code.

Our previous theoretical study (AFCRL-TR-75-0509) of the recombination kinetics of  $e + NO^+$  had been directed mainly toward the calculation of the energy (temperature) dependence of the recombination cross-section. The pertinent potential energy curves were calculated using ab initio CI methods and were defined to near-spectroscopic accuracy. An important problem is the determination of the branching into  $N(^4S)$  and  $N(^2D)$ , which has been shown by our studies to be governed by states of  $2\Sigma^+$  symmetry of NO. A calculation of the detailed branching from an initial recombination into the  $I\ 2\Sigma^+$  state of NO to atomic separations of  $N(^4S) + O(^3P)$  and  $N(^2D) + O(^3P)$  was the principal thrust of our CY79 research effort.

Calculations of the branching ratio between the  $A^2\Sigma^+$  and  $I^2\Sigma^+$  molecular states of NO have been carried out for the dissociative-recombination of  $e + NO^+$ . The dominant recombination channels for this reaction for incident energies less than  $\sim 0.5$  eV, are the  $B^2\Pi$ ,  $L^2\Pi$  and  $B'\ 2\Lambda$  states of NO. However,  $\sim 20\%$  of the recombination occurs along the  $2\Sigma^+$  symmetry path. Our calculated diabatic potential curves for  $2\Sigma^+$  symmetry indicate a maximum Hamiltonian interaction term,  $H_{ij}$ , of  $270\ cm^{-1}$  for an internuclear separation of 2.842 bohrs. Using a full close-coupling code, we calculate that the coupling cross-section between the  $I\ 2\Sigma^+$  and  $A\ 2\Sigma^+$  states of NO never exceeds  $10^{-20}\ cm^2$  for collisional energies  $\leq 2.0$  eV. The recombination along the  $I\ 2\Sigma^+$  channel thus follows a diabatic reaction path and we predict exclusively that  $N[^2D] + O [^3P]$  are the atomic products of dissociative-recombination of  $e + NO^+$ .

Preliminary studies of the  $O^+ + N_2$  reaction were carried out to examine likely reaction pathways. The molecular correlation diagram of  $N_2O$  has been constructed for collision energies up to 6.16 eV, and including all channels below  $O^+[^4S] + N_2 [A^3\Sigma_u^+]$ . Spin correlations indicate that the lowest adiabatic surface should be of quartet symmetry. Previous studies, using SCF procedures, produced a co-linear reaction path ( $4\Sigma^-$ ) which exhibited a barrier height of approximately 7 eV. In contrast, the best experimental estimate of the barrier in this system is  $\sim 0.2$  eV.

Our preliminary studies indicate that the spin-recoupling that occurs in going from reactants to products is not adequately represented with SCF or MC-SCF frameworks. Detailed calculations are required to estimate the spin-correlation errors and such studies are proposed as a logical extension of our present research efforts.

Theoretical Research Investigation Upon  
Reaction Rates to the Nitric Oxide  
Positive Ion

TABLE OF CONTENTS

	<u>Page</u>
INTRODUCTION . . . . .	1
CURRENT STATUS OF QUANTUM MECHANICAL METHODS FOR DIATOMIC SYSTEMS . . .	3
METHOD OF APPROACH . . . . .	6
1. Levels of Approximation . . . . .	6
2. Spin and Symmetry . . . . .	6
3. Method of <u>Ab Initio</u> Calculation . . . . .	7
4. Molecular Integrals . . . . .	10
5. Configuration Selection . . . . .	10
6. Charge-Transfer Calculation . . . . .	10
7. Rotationally Induced Transition . . . . .	14
8. Dissociative - Recombination Rate . . . . .	17
DISCUSSION OF RESULTS . . . . .	25
REFERENCES . . . . .	32
FIGURES . . . . .	39
TABLES . . . . .	46
DISTRIBUTION LIST . . . . .	52

Accession For	
NTIS GRA&I	
DTIC TAB	
Unannounced	
Justification	
X	
By _____	
Distribution	
Availability Codes	
Dist	Avail and/or Special
A	

LIST OF ILLUSTRATIONS

<u>Figure</u>		<u>Page</u>
1	Potential Energy Curves of NO Leading to Dissociative - Recombination in $\text{NO}^+$	39
2	Dissociative - Recombination Rate Coefficient, $\text{cm}^3/\text{sec}$	40
3	Branching Ratio Analysis	41
4	Interaction Potential for $\text{NO}(\text{A}^2\Sigma^+ - \text{I}^2\Sigma^+)$	42
5	Total Recombination Cross-Section, $\text{cm}^2$	43
6	Vector Coupling Diagram for Electron Spin	44
7	Co-linear Reaction Pathway for $\text{O}^+ + \text{N}_2$	45

LIST OF TABLES

<u>Table</u>	<u>Page</u>
1    Calculated Dissociative-Recombination Rate Coefficients $\alpha$ (Te, v = 0), cm <sup>3</sup> /sec . . . . .	46
2    Calculated Dissociative-Recombination Rate Coefficients $\alpha$ (Te, v = 2), cm <sup>3</sup> /sec . . . . .	47
3    Calculated Cross-Section for Dissociative-Recombination, cm <sup>2</sup> (v = 0) . . . . .	48
4    Diabatic $^2\Sigma^+$ Potential Energy Curves for NO . . . . .	49
5    Excitation Cross-Sections for $^2\Sigma^+$ States of NO . . . . .	50
6    Molecular Correlation Diagram for $O^+ + N_2 \rightarrow NO^+ + N$ . . . . .	51

## INTRODUCTION

The release of certain chemical species into the upper atmosphere results in luminous clouds that display the resonance electronic-vibrational-rotation spectrum of the released species. Such spectra are seen in rocket releases of chemicals for upper atmospheric studies and upon reentry into the atmosphere of artificial satellites and missiles. Of particular interest in this connection is the observed spectra of certain metallic oxides and air diatomic and triatomic species. From band intensity distribution of the spectra, and knowledge of the f-values of electronic and vibrational transitions, the local conditions of the atmosphere can be determined (Ref. 1).

Present theoretical efforts which are directed toward a more complete and realistic analysis of the transport equations governing atmospheric relaxation, including chemical effects, and the propagation of artificial disturbances require detailed information on atomic and ionic reaction rates and on thermal opacities and LWIR absorption in regions of temperature and pressure where molecular effects are important (Refs. 2 and 3). Although various experimental techniques have been employed for both atomic and molecular systems, theoretical studies have been largely confined to an analysis of the properties (bound-bound, bound-free and free-free) of atomic systems (Refs. 4 and 5). This has been due in large part to the unavailability of reliable wavefunctions for diatomic molecular systems, and particularly for excited states or states of open-shell structures. More recently, (Refs. 6-9) reliable theoretical procedures have been prescribed for such systems which have resulted in the development of practical computational programs.

The theoretical analysis of atmospheric reactions requires the knowledge of the electronic structure of atoms, ions and small molecular clusters of nitrogen and oxygen and the interaction of water or other small molecules with these clusters. Knowledge of the chemistry of metal oxide species, which might be present in a contaminated atmosphere, is also desired. In addition the basic collisional processes involving electrons, ions and neutral particles must be understood to evaluate the dynamic effects of the chemistry of the atmosphere. One important reaction is charge transfer in  $N^+ + O \rightarrow N + O^+$ . This has been studied experimentally by Neynaber (Refs. 10 and 71) at collision energies between 0.5 eV and 25 eV but low energy (< 0.5 eV) data are apparently extremely difficult to measure.

Because of the difficulty of conducting experiments to measure the appropriate cross sections for many thermal energy atmospheric processes, the development of a sound theoretical method for calculating low-energy cross sections appears necessary. Although relatively little work of this nature has been done in the past, enough theoretical work is available to indicate that the development of such procedures can be made practical, particularly if good wave functions and potential energy curves are available for the interacting species.

Earlier research (Technical Report No. AFWL-TR-72-1) was undertaken to assess the reliability of theoretically predicting diatomic transition probabilities. The systems studied under this program included the nitrogen first positive system, the oxygen Schumann-Runge system and the nitric oxide beta system. In addition, a preliminary study of theoretical techniques was undertaken for predicting cross sections for collisions involving electrons and molecular ions. Large two-body electron-ion recombination coefficients have been observed in recombining plasmas, both in the laboratory and in the upper atmosphere. Bates was the first to suggest that these large recombination coefficients could be explained in terms of the recombination of electrons and molecular ions in a process called dissociative recombination; whereas, the coefficients associated with the recombination of electrons and atomic ions were expected to be several orders of magnitude smaller.

As an extension of our collisional studies of  $N^+ + O$ , an examination of the branching ratios in the dissociative-recombination of  $e + NO^+ \rightarrow N[{}^2D, {}^4S] + O$  was carried out. This study utilized the results of our previous research of the electronic structure of  $NO^+$  and  $NO$ . In addition, a preliminary examination of the ion-molecule reaction,  $O^+ + N_2 \rightarrow NO^+ + N$  was carried out to access possible reaction pathways. The goal of this entire research program was to develop technical information concerning these systems which is relevant to DNA interests in upper atmospheric reactions.

## CURRENT STATUS OF QUANTUM MECHANICAL METHODS FOR DIATOMIC SYSTEMS

The application of quantum mechanical methods to the prediction of electronic structure has yielded much detailed information about atomic and molecular properties (Ref. 7). Particularly in the past few years, the availability of high-speed computers with large storage capacities has made it possible to examine both atomic and molecular systems using an ab initio approach, wherein no empirical parameters are employed (Ref. 11). Ab initio calculations for diatomic molecules employ a Hamiltonian based on the non-relativistic electrostatic interaction of the nuclei and electrons, and a wavefunction formed by antisymmetrizing a suitable many-electron function of spatial and spin coordinates. For most applications it is also necessary that the wavefunction represent a particular spin eigenstate and that it have appropriate geometrical symmetry. Nearly all the calculations performed to date are based on the use of one-electron orbitals and are of two types: Hartree-Fock or configuration interaction (Ref. 8).

Hartree-Fock calculations are based on a single assignment of electrons to spatial orbitals, following which the spatial orbitals are optimized, usually subject to certain restrictions. Almost all Hartree-Fock calculations have been subject to the assumption that the diatomic spatial orbitals are all doubly occupied, as nearly as possible, and are all of definite geometrical symmetry. These restrictions define the conventional, or restricted, Hartree-Fock (RHF) method (Refs. 12 and 13). RHF calculations can be made with relatively large Slater-type orbital (STO) basis sets for diatomic molecules with first or second-row atoms, and the results are convergent in the sense that they are insensitive to basis enlargement. The RHF model is adequate to give a qualitatively correct description of the electron interaction in many systems, and in favorable cases can yield equilibrium interatomic separations and force constants. However, the double-occupancy restriction makes the RHF method inappropriate in a number of circumstances of practical interest. In particular, it cannot provide potential curves for molecules dissociating into odd-electron atoms (e.g., NO at large internuclear separation), or into atoms having less electron pairing than the original molecule [e.g.,  $O_2 \xrightarrow{g} O(^3P)$ ]; it cannot handle excited states having unpaired electrons (e.g., the  $^3\Sigma$  states of  $O_2$  responsible for the Schumann-Runge bands); and, in general, it gives misleading results for molecules in which the extent of electron correlation changes with internuclear separation.

Configuration-interaction (CI) methods have the capability of avoiding the limitations of the RHF calculations. If configurations not restricted to doubly-occupied orbitals are included, a CI can, in principle, converge to an exact wave-function for the customary Hamiltonian. However, many CI calculations have in fact been based on a restriction to doubly-occupied

orbitals and therefore retain many of the disadvantages of the RHF method (Ref. 8). The use of general CI formulations involves three considerations, all of which have been satisfactorily investigated: the choice of basis orbitals, the choice of configurations (sets of orbital assignments), and the specific calculations needed to make wavefunctions describing pure spin states (Ref. 6). The first consideration is the art associated with quantum mechanical electronic structure calculations. Many methods (iterative NSO, perturbation selection, first order CI, etc.) have been advocated for the optimum choice of configurations. There are no firm rules at present and the optimum choice is a strong function of the insight of the particular research investigator. The last consideration, proper spin and symmetry projection, has proved difficult to implement, but computer programs have been developed for linear projection algebra at this Center, and the CI method has been found of demonstrable value in handling excited states and dissociation processes which cannot be treated with RHF techniques.

Either of the above described methods for ab initio calculations reduces in practice to a series of steps, the most important of which are the evaluation of molecular integrals, the construction of matrix elements of the Hamiltonian, and the optimization of molecular orbitals (RHF) or configuration coefficients (CI). For diatomic molecules, these steps are all comparable in their computing time, so that a point has been reached where there is no longer any one bottleneck determining computation speed. In short, the integral evaluation involves the use of ellipsoidal coordinates and the introduction of the Neumann expansion for the interelectronic repulsion potential (Ref. 14); the matrix element construction depends upon an analysis of the algebra of spin eigenfunctions (Ref. 15); and the orbital or configuration optimization can be carried out by eigenvalue techniques (Refs. 16, 17). All the steps have by now become relatively standard and can be performed efficiently on a computer having 65,000 to 130,000 words of core storage, a cycle time in the microsecond range, and several hundred thousand words of peripheral storage.

Both the RHF and CI methods yield electronic wavefunctions and energies as a function of the internuclear separation, the RHF methods for one state, and the CI method for all states considered. The electronic energies can be regarded as potential curves, from which may be deduced equilibrium internuclear separations, dissociation energies, and constants describing vibrational and rotational motion (including anharmonic and rotation-vibration effects). It is also possible to solve the Schrödinger equation for the motion of the nuclei subject to the potential curves, to obtain vibrational wavefunctions for use in transition probability calculations. The electronic wavefunctions themselves can be used to estimate dipole moments of individual electronic states, transition moments between different electronic states, and other properties. While all of the calculations described in this

paragraph have been carried out on some systems, the unavailability of good electronic wavefunctions and potential curves has limited actual studies of most of these properties to a very small number of molecules.

## METHOD OF APPROACH

Central to these studies are the actual quantum-mechanical calculations which must be carried out for the molecular species. For added clarity, various aspects of these calculations are discussed in individual subsections.

### 1. Levels of Approximation

Much evidence on diatomic and polyatomic systems indicates the near adequacy of a minimum Slater-type-orbital (STO) basis for constructing molecular wavefunctions (Refs. 18 and 19). This means inner-shell and valence-shell STO's of quantum numbers appropriate to the atoms (1s, 2s, 2p for C, N, O; 1s for H). The main deficiency of the minimum basis set is in its inability to describe polarization of  $\pi$  orbitals in atoms adjacent to H atoms, and successful calculations usually result if one (or a set) of p orbitals is supplied for each H atom. Values of the screening parameters  $\zeta$  for each orbital can either be set from atomic studies or optimized in the molecule; the later approach is indicated for studies of maximum precision. When high chemical accuracy is required, as for the detailed studies of the ground state of a system, a more extended basis should be used. Double-zeta plus polarization functions or optimized MO's usually are required.

The chosen basis sets give good results only when used in a maximally flexible manner. This implies the construction of CI wavefunctions with all kinds of possible orbital occupancies, so that the correlation of electrons into overall states can adjust to an optimum form at each geometrical conformation and for each state. Except when well-defined pairings exist for as many electrons as possible, a single-configuration study (even of Hartree-Fock quality) will be inadequate.

### 2. Spin and Symmetry

Proper electronic states for systems composed of light atoms should possess definite eigenvalues of the spin operator  $S^2$  as well as an appropriate geometrical symmetry. The geometrical symmetry can be controlled by the assignment of orbitals to each configuration, but the spin state must be obtained by a constructive or projective technique. Formulas have been developed (Ref. 15) for projective construction of spin states from orthogonal orbitals, and programs implementing these formulas have for several years been in routine use at UTRC.

One of the least widely appreciated aspects of the spin-projection problem is that the same set of occupied spatial orbitals can sometimes be coupled to give more than one overall state of given S quantum number. It is necessary to include in calculations all such spin couplings, as the optimum coupling will continuously change with changes in the molecular conformation. This is especially important in describing degenerate or near-degenerate excited electronic states.

### 3. Method of Ab Initio Calculation

A spin-free, nonrelativistic, electrostatic Hamiltonian is employed in the Born-Oppenheimer approximation. In systems containing atoms as heavy as N or O, this approximation is quite good for low-lying molecular states. For a diatomic molecule containing n electrons, the approximation leads to an electronic Hamiltonian depending parametrically on the internuclear separation, R:

$$\mathcal{H}(R) = -\frac{1}{2} \sum_{i=1}^n \nabla_i^2 - \sum_{i=1}^n \frac{Z_A}{r_{iA}} - \sum_{i=1}^n \frac{Z_B}{r_{iB}} + \frac{Z_A Z_B}{R} + \sum_{i>j \geq 1}^n \frac{1}{r_{ij}} \quad (1)$$

where  $Z_A$  and  $Z_B$  are the charges of nuclei A and B, and  $r_{iA}$  is the separation of electron i and nucleus A.  $\mathcal{H}$  is in atomic units (energy in Hartrees, length in Bohrs).

Electronic wavefunctions  $\psi(R)$  are made to be optimum approximations to solutions, for a given R, of the Schrödinger equation

$$\mathcal{H}(R)\Psi(R) = E(R)\Psi(R) \quad (2)$$

by invoking the variational principle

$$\delta W(R) = \delta \frac{\int \Psi^*(R) \mathcal{H}(R) \Psi(R) d\tau}{\int \Psi^*(R) \Psi(R) d\tau} \quad (3)$$

The integrations in Eq. (3) are over all electronic coordinates and the stationary values of  $W(R)$  are approximations to the energies of states described by the corresponding  $\psi(R)$ . States of a particular symmetry are studied by restricting the electronic wavefunction to be a projection of the appropriate angular momentum and spin operators. Excited electronic states corresponding

to a particular symmetry are handled by construction of configuration-interaction wavefunctions of appropriate size and form.

The specific form for  $\psi(R)$  may be written

$$\Psi(R) = \sum_{\mu} c_{\mu} \Psi_{\mu}(R) \quad (4)$$

where each  $\psi_{\mu}(R)$  is referred to as a configuration, and has the general structure

$$\Psi_{\mu}(R) = A \mathcal{O}_S \prod_{i=1}^n \Psi_{\mu i}(\mathbf{r}_i, R) \theta_M \quad (5)$$

where each  $\psi_{\mu i}$  is a spatial orbital,  $A$  is the antisymmetrizing operator,  $\mathcal{O}_S$  is the spin-projection operator for spin quantum number  $S$ , and  $\theta_M$  is a product of  $\alpha$  and  $\beta$  one-electron spin functions of magnetic quantum number  $M$ . No requirement is imposed as to the double occupancy of the spatial orbital, so Eqs. (4) and (5) can describe a completely general wavefunction.

In Hartree-Fock calculations  $\psi(R)$  is restricted to a single  $\psi_u$  which is assumed to consist as nearly as possible of doubly-occupied orbitals. The orbitals  $\psi_{\mu i}$  are then selected to be the linear combinations of basis orbitals best satisfying Eq. (3). Writing

$$\Psi_{\mu i} = \sum_{\nu} a_{\nu i} \chi_{\nu} \quad (6)$$

the  $a_{\nu i}$  are determined by solving the matrix Hartree-Fock equations

$$\sum_{\nu} F_{\lambda \nu} a_{\nu i} = \epsilon_i \sum_{\nu} S_{\lambda \nu} a_{\nu i} \text{ (each } \lambda \text{)} \quad (7)$$

where  $\epsilon_i$  is the orbital energy of  $\psi_{\mu i}$ .

The Fock operator  $F_{\lambda \nu}$  has been thoroughly discussed in the literature (Ref. 12) and depends upon one- and two-electron molecular integrals and upon the  $a_{\nu i}$ . This makes Eq. (7) nonlinear and it is therefore solved iteratively. UTRC has developed programs for solving Eq. (7) for both closed and open-shell systems, using basis sets consisting of Slater-type atomic orbitals. Examples of their use are in the literature (Ref. 6).

In configuration interaction calculations, the summation in Eq. (4) has more than one term, and the  $c_\nu$  are determined by imposing Eq. (3), to obtain the secular equation

$$\sum_\nu (H_{\mu\nu} - w S_{\mu\nu}) c_\nu = 0 \quad (\text{each } \mu) \quad (8)$$

where

$$H_{\mu\nu} = \int \Psi_\mu^*(R) dH(R) \Psi_\nu(R) d\tau$$

$$S_{\mu\nu} = \int \Psi_\mu^*(R) \Psi_\nu(R) d\tau \quad (9)$$

Equation (7) is solved by matrix diagonalization using either a modified Givens method (Ref. 16) or a method due to Shavitt (Ref. 17).

The matrix elements  $H_{\mu\nu}$  and  $S_{\mu\nu}$  may be reduced by appropriate operator algebra to the forms

$$H_{\mu\nu} = \sum_P \epsilon_P \left\langle \theta_M | O_S P | \theta_M \right\rangle \left\langle \prod_{i=1}^n \Psi_{\mu i}(r_i, R) \right| dH(R) P \left| \prod_{i=1}^n \Psi_{\nu i}(r_i, R) \right\rangle \quad (10)$$

$$S_{\mu\nu} = \sum_P \epsilon_P \left\langle \theta_M | O_S P | \theta_M \right\rangle \left\langle \prod_{i=1}^n \Psi_{\mu i}(r_i, R) \right| P \left| \prod_{i=1}^n \Psi_{\nu i}(r_i, R) \right\rangle \quad (11)$$

where  $P$  is a permutation and  $\epsilon_P$  its parity. The sum is over all permutations.  $\langle \theta_M | s P | \theta_M \rangle$  is a "Sanibel coefficient" and the remaining factors are spatial integrals which can be factored into one- and two-electron integrals. If the  $\Psi_{\mu i}$  are orthonormal, Eqs. (10) and (11) become more tractable and the  $H_{\mu\nu}$  and  $S_{\mu\nu}$  may be evaluated by explicit methods given in the literature (Ref. 15). Computer programs have been developed for carrying out this procedure, and they have been used for problems containing up to 40 total electrons, 10 unpaired electrons, and several thousand configurations.

The CI studies described above can be carried out for any orthonormal set of  $\Psi_{\mu i}$  for which the molecular integrals can be calculated. Programs developed by UTRC make specific provision for the choice of the  $\Psi_{\mu i}$  as Slater-type atomic orbitals, as symmetry molecular orbitals, as Hartree-Fock orbitals, or as more arbitrary combinations of atomic orbitals.

#### 4. Molecular Integrals

The one- and two-electron integrals needed for the above described method of calculation are evaluated for STO's by methods developed by the present investigators (Ref. 20). All needed computer programs have been developed and fully tested at UTRC.

#### 5. Configuration Selection

Using a minimum basis plus polarization set of one-electron functions, a typical system can have of the order of  $10^4$  configurations in full CI (that resulting from all possible orbital occupancies). It is therefore essential to identify and use the configurations describing the significant part of the wavefunction. There are several ways to accomplish this objective. First, one may screen atomic-orbital occupancies to eliminate those with excessive formal charge. Alternatively, in a molecular-orbital framework one may eliminate configurations with excessive numbers of anti-bonding orbitals. A third possibility is to carry out an initial screening of configurations, rejecting those whose diagonal energies and interaction matrix elements do not satisfy significance criteria. Programs to sort configurations on all the above criteria are available at UTRC.

Other, potentially more elegant methods of configuration choice involve formal approaches based on natural-orbital (Ref. 21) or multiconfiguration SCF (Ref. 8) concepts. To implement the natural-orbital approach, an initial limited-CI wave-function is transformed to natural-orbital form, and the resulting natural orbitals are used to form a new CI. The hoped-for result is a concentration of the bulk of the CI wavefunction into a smaller number of significant terms. The multiconfiguration SCF approach is more cumbersome, but in principle more effective. It yields the optimum orbital choice for a pre-selected set of configurations. This approach works well when a small number of dominant configurations can be readily identified.

It should be emphasized that the problem of configuration choice is not trivial, and represents an area of detailed study in this research. The existence of this problem causes integral evaluation to be far from a unique limiting factor in the work.

#### 6. Charge-Transfer Calculations

Even though low-energy atom-atom reactions play an important role in many physical processes, until recently comparatively little effort had been devoted to acquiring a knowledge of the appropriate cross sections. In the

past, both theoreticians and experimental physicists have found it easier to study high-energy collisions. At these energies, the two colliding particles preserve their identities, and it is possible to treat the interaction between them as a perturbation. There is no guarantee that this procedure, known as the Born approximation, will always converge to the correct result (Ref. 22). As the energy of the colliding particles decreases, it is necessary to take account of the distortion these particles undergo during the collision. The method of perturbed stationary states was developed for calculating charge transfer and electronic excitation cross sections in relatively slow collisions between heavy particles (Ref. 23). The method has been presented in both wave and impact parameter formalisms. In the first of these, the entire system is treated quantum-mechanically, while in the latter the nuclei are assumed to behave as classical particles, traveling along straight line trajectories, and the time-dependent Schrödinger equation is solved to calculate the probability of various types of electronic transitions (Refs. 24, 25 and 26). Forcing the particles to travel along straight lines limits the validity of the impact parameter method to collisions of several hundred electron-volts or greater (Ref. 27). The wave formulation of the method of perturbed stationary states appears to be one practical method of calculating thermal-energy charge-exchange cross sections. A semi-classical close-coupling method (Ref. 28), based on an average scaling procedure, also offers utility for low to intermediate collision energies.

The use of the wave formalism to study charge-transfer reactions at thermal energies dates back to Massey and Smith's pioneering study of  $\text{He}^+ + \text{He}$  thermal low-energy scattering (Ref. 29). Strictly speaking, their theory is applicable only to resonant charge transfer reactions,  $\text{A} + \text{A}^+ \rightarrow \text{A}^+ + \text{A}$ ; however, it can be generalized to study nonresonant charge-transfer reactions as well as charge transfer into excited states. If the origin of coordinates is located at the center of mass of the nuclei of the colliding atoms, the Schrödinger equation for an atomic collision can be written in center of mass coordinates as

$$(H - E) X(\bar{r}, \bar{R}) = (H_0 - \frac{\hbar^2}{2M} \nabla_{\bar{R}}^2 - \frac{\hbar^2}{2M} \sum_i \sum_j \nabla_i \cdot \nabla_j - E) X(\bar{r}, \bar{R}) = 0 \quad (12)$$

where  $\bar{r}$  represents the position of the electrons,  $\bar{R}$  is the vector joining A to B,  $H_0$  is the Hamiltonian for the system when the nuclei are held fixed,  $M$  is the reduced mass of the two nuclei,  $M$  is the sum of the nuclear masses, and  $E$  is the internal energy of the system, including the electronic energy. Ignoring heavy particle kinetic energy terms in the center of mass system results in a modified form of the adiabatic approximation (Ref. 30) and yields perturbed molecular eigenfunctions  $\psi_n(\bar{r}, \bar{R})$  which satisfy the equation

$$(H_0 - \frac{\hbar^2}{2M} \sum_i \sum_j \nabla_i \cdot \nabla_j) \psi_n(\vec{r}, \vec{R}) = \epsilon_n(R) \psi_n(\vec{r}, \vec{R}) \quad (13)$$

Here  $\epsilon_n(R)$  is an electronic energy level of the molecule perturbed somewhat by the appearance of the cross terms. The wave function describing the colliding system,  $X(\vec{r}, \vec{R})$  can be expanded as

$$X(\vec{r}, \vec{R}) = \sum_n \psi_n(\vec{r}, \vec{R}) F_n(\vec{R}) \quad (14)$$

The various scattering cross sections are determined by the asymptotic behavior of the  $F_n(\vec{R})$ . These functions are determined by substituting the expansion Eq. (14) into Eq. (12). Making use of the orthogonality of the molecular eigenfunctions, it is easy to derive the following set of coupled differential equations for the  $F_n(\vec{R})$

$$\left( -\frac{\hbar^2}{2M} \nabla_{\vec{R}}^2 + V_n(\vec{R}) - \frac{\hbar^2 k_n^2}{2M} \right) F_n(\vec{R}) = \sum_m \frac{\hbar^2}{2M} \left\{ \langle \psi_n | \nabla_{\vec{R}}^2 | \psi_m \rangle F_m(\vec{R}) \right. \\ \left. + 2 \langle \psi_n | \nabla_{\vec{R}} | \psi_m \rangle \cdot \nabla_{\vec{R}} F_m(\vec{R}) \right\} \quad (15)$$

where  $V_n(R)$  and  $\hbar^2 k_n^2 / 2M$  are the potential and kinetic energies of particles in the  $n^{\text{th}}$  channel. Many of the difficulties associated with trying to calculate thermal energy cross sections emanate from trying to derive and solve this infinite set of coupled partial differential equations. Until recently, the biggest obstacle in the calculation of low-energy cross sections has been the inability of theorists to develop accurate molecular eigenfunctions. For those problems for which the molecular eigenfunctions were available, the agreement between theory and experiment has been very reasonable for the amount of computational effort involved. This is true for spin exchange and excitation transfer reactions as well as resonance charge transfer reactions (Refs. 31-35).

Although the molecular wave functions and energies available in the past have not been sufficiently accurate to permit extension of the wave formalism to systems having more than about four electrons, recent advances in calculational techniques, especially for two-center systems, have largely overcome this problem. In particular, recent studies have demonstrated the possibility of producing highly accurate adiabatic electronic wave functions for systems containing as many as 40 electrons (Refs. 6, 36-38). The availability of these small but flexible wave functions, which have the property of connecting

with the correct separated atomic states, increases substantially the chances for successful and practical calculations of cross sections using the perturbed stationary state technique. This is especially true of charge transfer into excited states, where a knowledge of a number of the low-lying excited states is required.

Even with a reasonable number of the molecular eigenfunctions, the problem of calculating cross sections is far from solved; this is especially true of charge or excitation transfer into excited states. Many of the existing studies of symmetric resonance reactions are based on the two-state approximation which limits the number of terms in the expansion Eq. (14) to two. Under these conditions, the coupling terms on the right-hand side of Eq. (15) vanish (Ref. 39). We have, then, only to solve two partial differential equations, instead of a system of coupled equations. The situation is not as simple, however, for nonsymmetric reactions or for high-energy collisions involving excitation. For these problems, the coupling terms are the source of the transition and the coupled differential equations have to be solved directly.

While a great deal of effort has gone into deriving formal theories of inelastic and rearrangement collisions, relatively little work has gone into trying to solve the resulting equations. This is especially true of low-energy collisions, where the lack of good molecular wave functions has prevented people from evaluating the terms coupling the different channels. Previous studies which were part of the UTRC research program in the electronic structure of atoms and molecules have been devoted to calculating matrix elements similar to some of the terms coupling the electronic and nuclear motion. Some of the required work involves calculating derivatives of the electronic wave functions with respect to the internuclear distance. This task is made simpler by the use of compact but flexible wave functions such as those studied previously at this center.

The biggest obstacle to calculating low-energy cross sections is the solution of the infinite system of coupled partial differential equations describing the scattering (Eq. 15). The physics of the problem usually serves as a guide to truncating these equations to a system of finite order. A partial wave expansion of the  $F_n(\bar{R})$  leaves a large number of sets of coupled differential equations (Refs. 40 and 41). Since the number of equations increases as the collision energy increases, there is no single method for solving these equations. At thermal energies, a direct numerical integration of these equations is feasible (Refs. 42 and 43). At higher energies, when inelastic collisions and charge transfer into excited states becomes important, the trajectories of the incident and scattered particles may be nearly classical (Ref. 44). Under these conditions, it is often possible to use the W. K. B. wave function to obtain approximate solutions to these equations (Ref. 45).

## 7. Rotationally Induced Transition

Our studies of the electronic states of  $\text{NO}^+$  which are important in the  $\text{N}^+ + \text{O} \rightarrow \text{N} + \text{O}^+$  charge transfer reaction led primarily to consideration of the  ${}^5\Sigma^+$  and  ${}^5\Pi$  states of this molecular ion. The dominant reactant channel was found to be the lowest  ${}^5\Pi$  state, which is bound, and the connecting charge transfer channel which has  ${}^5\Sigma^+$  symmetry. For near-adiabatic collisions, this type of system can be handled using a semi-classical approach, directly solving the second order differential equations which couple the adiabatic levels, here of different angular momentum.

The adiabatic states  $\psi_1(\underline{r}, R)$  and  $\psi_2(\underline{r}, R)$  are eigenstates of the non-relativistic Hamiltonian,  $\mathcal{H}$ , for a fixed internuclear separation,  $R$ . We have

$$\mathcal{H}\phi_i(\underline{r}, R) = \epsilon_i\phi_i(\underline{r}, R) \quad i = 1, 2 \quad (16)$$

In the two-state approximation we have, using impact parameter formulation,

$$\begin{aligned} \psi &= c_1(t) \phi_1(\underline{r}, R) e^{-i/\hbar \int_0^t \epsilon_1 d\tau} \\ &\quad + c_2(t) \phi_2(\underline{r}, R) e^{-i/\hbar \int_0^t \epsilon_2 d\tau} \end{aligned} \quad (17)$$

where  $R = R(t)$  and is defined by the collision trajectory.

We now require the inner product of  $\psi$  and  $\phi_i$  to vanish over the electronic coordinates

$$\langle \phi_1 | \mathcal{H} - i\hbar \frac{\partial}{\partial t} | \psi \rangle = 0 \quad (18a)$$

$$\langle \phi_2 | \mathcal{H} - i\hbar \frac{\partial}{\partial t} | \psi \rangle = 0 \quad (18b)$$

Combining Eqs. (16), (17), and (18), we have

$$\left[ \frac{\partial c_1}{\partial t} + c_1 \langle \phi_1 \left| \frac{\partial \phi_1}{\partial t} \right. \rangle \right] e^{-i/\hbar \int_0^t \epsilon_1 d\tau} \quad (19a)$$

$$+ c_2 \langle \phi_1 \left| \frac{\partial \phi_2}{\partial t} \right. \rangle e^{-i/\hbar \int_0^t \epsilon_2 d\tau} = 0$$

$$\left[ \frac{\partial c_2}{\partial t} + c_2 \langle \phi_2 | \frac{\partial \phi_2}{\partial t} \rangle \right] e^{-i/\hbar \int_0^t \epsilon_2 d\tau} + c_1 \langle \phi_2 | \frac{\partial \phi_1}{\partial t} \rangle e^{-i/\hbar \int_0^t \epsilon_1 d\tau} = 0 \quad (19b)$$

Converting from differentiation with respect to time, to velocity and angular momentum, we have

$$\frac{\partial \phi_i}{\partial t} = \frac{\partial R}{\partial t} \frac{\partial \phi_i}{\partial R} + \frac{i}{\hbar} \frac{\partial V_\theta}{\partial t} L_T \phi_i; \frac{\partial V_\theta}{\partial t} L_T \phi_i \quad (20)$$

where  $V_\theta$  is the angular velocity of the internuclear axis and  $L_T$  is the angular momentum coupling operator. The first term on the RHS of Eq. (20) leads to the well known Landau-Zener (Ref. 46) solution for states of identical molecular symmetry. For such cases the second term in Eq. (20) vanishes.

For the system under study here, only the second term on the RHS of Eq. (20) contributes in Eqs. (19) and we are led to the following coupled equations,

$$\frac{\partial c_1}{\partial t} + \frac{i}{\hbar} \frac{\partial V_\theta}{\partial t} c_2 \langle \phi_1 | L_T | \phi_2 \rangle e^{-\frac{i}{\hbar} \int_0^t (\epsilon_2 - \epsilon_1) d\tau} = 0 \quad (21a)$$

$$\frac{\partial c_2}{\partial t} + \frac{i}{\hbar} \frac{\partial V_\theta}{\partial t} c_1 \langle \phi_2 | L_T | \phi_1 \rangle e^{-\frac{i}{\hbar} \int_0^t (\epsilon_1 - \epsilon_2) d\tau} = 0 \quad (21b)$$

Assuming a linear dependence of  $\epsilon$  on  $R$  near the crossing point of the collision, we have

$$\epsilon_2 - \epsilon_1 = b\hbar(R - R_x) = at \quad (22)$$

$$\alpha = \frac{V_R}{\hbar} \left. \frac{d(\epsilon_2 - \epsilon_1)}{dR} \right|_{R_x} \quad (23)$$

Assuming also that  $\langle \phi_1 | L_T | \phi_2 \rangle = \langle L_T \rangle$  is essentially constant over the dominant region of the collision, we have

$$\frac{\partial C_1}{\partial t} + \frac{iW \langle L_T \rangle}{\hbar} C_2 e^{-\frac{i}{\hbar} \int_0^t (\epsilon_2 - \epsilon_1) d\tau} = 0 \quad (24a)$$

$$\frac{\partial C_2}{\partial t} + \frac{iW \langle L_T \rangle}{\hbar} C_1 e^{-\frac{i}{\hbar} \int_0^t (\epsilon_1 - \epsilon_2) d\tau} = 0 \quad (24b)$$

Equations (24a) and (24b) have been solved numerically by Russek (Ref. 47) for the case of curve-crossing states with  $\Delta\Lambda = \pm 1$ . For small values of angular velocity, Russek shows that Eq. (24) reduces to a standard Landau-Zener form. For large velocities, the general solution of Eq. (24) must be employed.

## 8. Dissociative-Recombination Rate

The theory of the capture of an electron by a positive molecular ion has been developed for both direct attachment processes (Ref. 48), and for several possible indirect processes which involve the formation of an intermediate excited Rydberg state belonging to the molecular ion core configuration (Refs. 49-50). Let  $\psi_f(r, R)$  represent the continuum wavefunction describing the free electron with energy  $\epsilon$  plus the  $n-l$  electron bound system of the molecular ion. Let  $\psi_d(r, R)$  represent the wavefunction for an eigenstate of the neutral molecule which can be written, in the Born-Oppenheimer approximation, as the product of an electronic and nuclear wavefunction in the form

$$\psi_d(r, R) = \psi_d^{el}(r, R) \xi_d(R) \quad (25)$$

The cross section for electron capture in the dissociative-recombination is determined by the asymptotic form of the nuclear wavefunction  $\xi_d(R)$ . Let the incident flux of electrons per unit area be

$$\frac{k^2}{2\pi^2\hbar} \delta\epsilon \quad (26)$$

where  $\delta\epsilon$  is a measure of the energy spread of the incoming beam and  $k$  is the wave number associated with the incoming electron. The outgoing flux of atoms is given by

$$\frac{\hbar k \delta\epsilon}{\mu} |\xi_d(R)|^2 \quad (27)$$

where  $\frac{\hbar k}{\mu}$  is the relative velocity of the separating neutral atoms. Equations (26) and (27) yield for the cross section

$$\sigma(\epsilon, \Omega) = \frac{n}{4\pi} \frac{2\pi^2 \hbar^2 k}{\mu \epsilon^2} |\xi_d(R)|^2 \quad (28)$$

Equation (28) must finally be averaged over all rotational orientations as

$$\sigma(\epsilon) = \frac{1}{4\pi} \int \sigma(\epsilon, \Omega) d\Omega \quad (29)$$

Assuming that the total cross sections can be written as the product of a resonant capture cross section and a survival factor, in the form

$$\sigma(\epsilon) = \sigma_{cap}(\epsilon) S(\epsilon) \quad (30)$$

we have

$$\sigma_{\text{cap}}(\epsilon) = \frac{\pi^2 \hbar^2}{2m\epsilon} \left( \frac{\omega_{AB}}{\omega_{AB}^+} \right) \langle \psi_{AB}^+(\underline{r}, R, \epsilon) | V(R, \epsilon) | \psi_d(\underline{r}, R) \rangle^2 \quad (31)$$

where the factor  $\omega_{AB}/\omega_{AB}^+$  is the ratio of the electronic degeneracies of the neutral and ionic states, respectively. The capture width,  $\Gamma_c(R, \epsilon)$ , is determined by integrating over the coordinates of the electronic wavefunctions

$$\Gamma_c(R, \epsilon) = 2\pi \langle \psi_{AB}^{el+}(\underline{r}, R) f(\epsilon, \underline{r}, R) | d_{el} \cdot \epsilon | \psi_{AB}^{el}(\underline{r}, R) \rangle^2 \quad (32)$$

Thus, the capture cross section can be written as

$$\sigma_{\text{cap}}(\epsilon) = \frac{\pi^2 \hbar^2}{2m\epsilon} \left( \frac{\omega_{AB}}{\omega_{AB}^+} \right) \frac{1}{2\pi} \langle \xi_{AB}^+(R) \Gamma_c^{1/2}(R, \epsilon) | \xi_{AB}^-(R) \rangle^2 \quad (33)$$

or equivalently

$$\sigma(\epsilon) = \frac{\pi^2 \hbar^2}{2m\epsilon} \left( \frac{\omega_{AB}}{\omega_{AB}^+} \right) \langle \xi_{AB}^+(R) \psi_{AB}^{el+}(R) f(\epsilon, R) V(R, \epsilon) | \psi_d(R) \xi_{AB}^-(R) \rangle^2 \quad (34)$$

The nuclear wavefunction,  $\xi_{AB}$ , is energy normalized such that asymptotically

$$\xi_{AB} \sim \left( \frac{2\mu}{\hbar^2} \times \frac{1}{\pi k} \right)^{1/2} \sin(kr + \eta) \quad (35)$$

Equation (34) can be cast into the computational form

$$\sigma(\epsilon, V) \text{ cm}^3/\text{sec} = \frac{1.38188 \times 10^{-16}}{\epsilon \text{ (a.u)}} \left( \frac{\omega_{AB}}{\omega_{AB}^+} \right) \langle \xi_{AB}^V(R) | \frac{\Gamma_c^{1/2}(R, \epsilon)}{\sqrt{2\pi}} | \xi_{AB}^-(R) \rangle^2 \quad (36)$$

where the electron energy,  $\epsilon$ , and the capture width  $\Gamma_c$  are in atomic units.

Assuming a Maxwellian temperature distribution for the electrons, the rate coefficient can be written as

$$a_v(T_e) = \frac{2}{\sqrt{\pi}} \frac{1}{(kT_e)^{3/2}} \int_0^\infty \sigma(\epsilon, V) \times v_{el} \times e^{-\epsilon/kT_e} \epsilon^{1/2} d\epsilon \quad (37)$$

or equivalently

$$\alpha_V(T_e) = \frac{2\sqrt{2}}{\sqrt{\pi m(kT_e)^{3/2}}} \int_0^\infty \sigma(\epsilon, V) e^{-\epsilon/kT_e} d\epsilon \quad (38)$$

The capture width  $\Gamma_c$  can be calculated by examining the high numbers of the Rydberg series of neutral states which have the structure of a ground state molecular ion coupled to an electron in a diffuse hydrogenic orbital of large effective principal quantum numbers. A direct calculation of the capture width involves the knowledge of the continuum wavefunction for the electron as a function of the interparticle coordinates. This approach is computationally very difficult and at the present stage of development would probably lead to errors of at least the same magnitude as an extrapolation procedure of the corresponding neutral Rydberg states. An alternate procedure is given here which involves analyzing only bound state functions.

#### Evaluation of Electronic Transition Matrix Elements

One of the most difficult tasks in the calculation of the cross section for dissociative-recombination is the evaluation of electronic matrix elements of the form  $\langle \psi_{AB}^{el}(r, R) | \mathcal{H}_{el} - \epsilon | \psi_{AB}^{el+}(r, R) f(\epsilon, r, R) \rangle$  where  $\mathcal{H}_{el}$  is the total electronic Hamiltonian,  $\psi_{AB}^{el}(r, R)$  is the electronic wavefunction for the valence state, and  $\psi_{AB}^{el+}(r, R) f(\epsilon, r, R)$  is the continuum wavefunction with total electronic energy,  $\epsilon$ . Unlike the  $\psi_{AB}^{el}$  which correspond to bound electronic valence states, the  $\psi_{AB}^{el+}(r, R) f(\epsilon, r, R)$  do not vanish for large electron-molecular ion separations but have an oscillatory behavior. The direct evaluation of these wavefunctions involves the solution of a very complicated scattering problem, and cannot be directly accomplished by the standard variational methods. We have developed two independent methods to evaluate these matrix elements that do not require the direct solution of the electron-molecular ion scattering problem.

Since it is a straightforward process to evaluate matrix elements of the form  $\langle \psi_{AB}^{el} | \mathcal{H}_{el} - \epsilon | \psi_{n*}^{el}(-E_{n*}) \rangle$  where  $\psi_{n*}^{el}(-E_{n*})$  is the wavefunction for a bound Rydberg state, one way of estimating the threshold value of the continuum analogue of these integrals is to analytically continue the bound state matrix elements into the continuum. In performing this analytic continuation, one has to be careful to include a factor corresponding to the density of states,  $\sigma(E_{n*}) = dn/dE$ . While this factor is implicitly included in the normalization constant for the continuum wavefunctions, it has to be explicitly calculated for the bound state functions. To a first approximation, the energy of the Rydberg states is proportional to  $\frac{1}{n^2}$ , therefore, the density of states increases, approximately, as  $n^3$ . On the basis of these approximations, we have been able to estimate the bound-continuum matrix elements for low scattering energies.

We have derived a second extrapolation procedure to calculate the bound-continuum electronic matrix elements at higher energies. A common procedure in theoretical physics for converting a continuum or scattering problem to a finite eigenvalue problem is to enclose the system in a spherical shell of finite volume and require the wavefunction to vanish at the boundaries. Depending on the form of the scattering potential, there will be a finite number of bound or negative energy states, and an infinite number of positive energy states, all satisfying the same boundary conditions. If the radius of the spherical shell is large enough, these bound state wavefunctions will be a reasonable approximation to the exact wavefunctions for the bound states. For any bound state and the infinite number of discrete states, it is possible to estimate the value of any bound-continuum matrix elements by plotting values of the product of the square of these matrix elements, times a discrete density of states function  $\rho(E_n^*) = |1/(E_n - E_{n+1})|$ . If the radius of our imaginary sphere is large enough, the curve generated from this procedure should give reasonable values for these matrix elements.

We have derived a many electron version of this theory. A finite set of bound state functions, which has a large continuum contribution, is diagonalized with respect to the operator,  $\mathcal{H}_{el}$ . This special set of Rydberg functions is then used to generate a series of curves for values of the matrix elements  $\langle \psi_v^{el} | \mathcal{H}_{el} - \epsilon | \psi_B^{el} \rangle$ . A set of estimated values of these matrix elements is given in Table A for s-wave (sigma) scattering states of NO.

TABLE A

Energy*	$\rho(E) * \langle \psi_v^{el}   \mathcal{H}_{el} - \epsilon   \psi_B^{el} \rangle^2$
.73	8.31 E-06
2.59	1.43 E-06
4.16	2.36 E-06
6.32	2.72 E-06
10.91	6.52 E-08

\*energy in atomic units relative to NO<sup>+</sup>.

#### Indirect Models

An indirect model for calculating electron-molecular ion recombination coefficients can also be formulated. Here we postulate the formation of a collision complex (AB\*) during the collision and its subsequent decay to form A\*, B\*\*, or AB<sup>+</sup> + e (Refs. 49-51). The approaches differ by the nature of the (AB\*) complex. The high-energy approximation assumes that all of the energy of the incident electron goes into exciting one of the electrons in the AB<sup>+</sup> core, resulting in the capture of the incident electron into a doubly excited state of AB. This mechanism is unlikely to be applicable to

$\text{AB}^+$  recombination at thermal energies because of the energy required to promote an electron out of the  $\text{AB}^+$  core. A second approach is more applicable to thermal energy collisions, since it requires that the electron-molecular ion collision results in a vibrationally excited molecular ion which captures an electron in the Coulomb field of  $\text{AB}^+$ . This collision complex is equivalent to a vibrationally or rotationally excited Rydberg state of  $\text{AB}$ . Experimental evidence for the existence of such states and their autoionization has been independently obtained from photoionization spectra of  $\text{AB}$ , within a few electron volts of threshold (Ref. 52). With this model, the prediction of the atomic products of the recombination reaction reduces to calculating the Rydberg states of  $\text{AB}$  that are most likely to be populated during the initial recombination, and also those atomic states to which they subsequently decay.

As contrasted with the direct recombination process which is governed by the configuration interaction strength, the nonadiabatic coupling of the electron and nuclear motion is the dominant mechanism in both stages of the indirect recombination process. In the first stage, it is the vibrational (or rotational) excitation of the  $\text{AB}^+$  core which results in the initial capture of the incident electron. The subsequent decay of the collision complex is due to a transition to a repulsive molecular state which crosses the Rydberg state. It is then the nonadiabatic coupling of the electronic and nuclear motion which results in the transition between these two molecular states. Actually, it is the same term in the Hamiltonian for the entire molecular system that causes the key transition in both stages of the recombination process. This becomes obvious in the quantum mechanical formulation of the problem. A possible competing process for the decay of the  $\text{AB}^*$  complex is the radiative transition to lower-lying states of the molecule. The importance of this effect can be estimated from calculations of the band transition probabilities.

Implicit in this model of dissociative-recombination processes is the existence of three excited electronic states of  $\text{AB}$ . Since this recombination process is envisioned as occurring in two stages, we are concerned with only two of these states at a time. The state common to both stages of the recombination process is the highly excited Rydberg state ( $\text{AB}^*$ ), which is bound with respect to dissociation to  $\text{AB}^+$  and a free electron. For the calculation of the initial rate of recombination, a wavefunction for a continuum Rydberg state is needed. This wavefunction has the asymptotic behavior of a free electron moving in the field of  $\text{AB}^+$ .

To determine the transition rates in the two stages of the recombination process, it is necessary to identify the terms in the Hamiltonian that are responsible for the transition. The Hamiltonian for the complete molecular system with respect to the center of mass is

$$\mathcal{H} = \mathcal{H}_0 - \frac{\hbar^2}{2\mu} \nabla_{\mathbf{R}}^2 - \frac{\hbar^2}{2M} \sum_i \sum_j \nabla_i V_j \quad (39)$$

where  $R$  is the vector joining nucleus  $B$ ,  $\mathcal{H}_0$  is the Hamiltonian for the system where the nuclei are held fixed,  $\mu$  is the reduced mass of the two nuclei,  $M$  is the sum of the nuclear masses, and the summations extend over all of the electrons. Since all of the electronic eigenfunctions under discussion are implicitly dependent on the internuclear separation  $|R|$ , it is the term  $\mathcal{H} = -(\hbar^2/2\mu)\nabla_R^2$  which plays a dominant role in coupling the electronic and nuclear motion giving rise to the appropriate transition (Refs. 53-56). This becomes more obvious when we write the total wavefunction for the collision complex,  $AB^*$ , as

$$\psi_c = \chi_c(z_e, |R|) F_c(R) \quad (40)$$

where  $\chi_c(z_e, |R|)$  is the electronic wavefunction for the appropriate Rydberg state of  $AB$  at internuclear separation  $|R|$  and  $F_c(R)$  is the wavefunction associated with the vibration and rotation of the nuclei. In a similar manner, the total wavefunction associated with the repulsive state is

$$\psi_r = \chi_r(z_e, |R|) F_r(R) \quad (41)$$

where  $F_r(R)$  is the wavefunction for the nitrogen and oxygen atoms as they separate. With the use of Fermi's golden rule, the transition rate for the decay of the collision can be obtained by evaluating the matrix elements.

$$\tau^{-1} = \frac{2\pi}{\hbar} |\langle \psi_c | \mathcal{H}' | \psi_r \rangle|^2 \quad (42)$$

The initial rate of recombination into the highly excited Rydberg state of nitrogen can be calculated in a similar manner.

We now consider the problem of the evaluation of the matrix elements appearing in Eq. (42). The most obvious way of handling this is to employ a direct approach and evaluate all matrix elements directly by quadrature. This reduces the problem to the calculation of matrix elements of the form (Ref. 57).

$$\langle \chi_c(z_e, |R|) F_c(R) | \nabla_R^2 | \chi_r(z_e, |R|) F_r(R) \rangle \quad (43)$$

While this task is possible, some of the physics of the problem become obscure with this direct approach. This is more obvious if Eq. (43) is simplified to

$$\left\langle \chi_c(\underline{r}_e, |R|) F_c(R) \left| F_n \nabla_{\underline{R}}^2 \chi_n(\underline{r}_e, |R|) + 2 \nabla_{\underline{R}} \chi_n \cdot \nabla_{\underline{R}} F_n + \chi_n \nabla_{\underline{R}}^2 F_n \right. \right\rangle \quad (44)$$

Since the derivatives of  $F_n(R)$  with respect to the nuclear coordinates are much greater than those of  $\chi_c(r_e, R)$ , Eq. (44) reduces to

$$2 \left\langle \psi_c(\underline{r}_e, |R|) \nabla_{\underline{R}} \chi_n \right\rangle \left\langle F_c(R) \nabla_{\underline{R}} F_n(R) \right\rangle \quad (45)$$

which can be expanded as

$$\left\langle M_{Cn}(R) F_c \frac{\partial F_n}{\partial R} \right\rangle + \left\langle N_{CR}(R) F_c \frac{\partial F_n}{R \partial \theta} \right\rangle \quad (46)$$

where

$$M_{Cn} = 2 \left\langle \chi_c(\underline{r}_e, |R|) \frac{\partial \chi_n}{\partial R}(\underline{r}_e, |R|) \right\rangle \quad (47a)$$

$$N_{Cn} = 2 \left\langle \chi_c(\underline{r}_e, |R|) \frac{\partial \chi_n}{R \partial \theta}(\underline{r}_e, |R|) \right\rangle \quad (47b)$$

If  $\chi_c$  and  $\chi_n$  are both eigenfunctions of the electronic Hamiltonian, i.e.,

$$H_{el} \chi_c(\underline{r}_e, |R|) = \epsilon_c(R) \chi_c \quad (48a)$$

$$H_{el} \chi_n(\underline{r}_e, |R|) = \epsilon_n(|R|) \chi_n \quad (48b)$$

then

$$M_{Cn}(R) = \frac{2}{\epsilon_n(R) - \epsilon_c(R)} \left\langle \chi_c(\underline{r}_e, |R|) \left| \frac{Z_B}{R_B^3} \chi_n \right. \right\rangle_{el} Z_B \quad (49a)$$

$$N_{Cn}(R) = \frac{2}{\epsilon_n(R) - \epsilon_c(R)} \left\langle \chi_c(\underline{r}_e, |R|) \left| \frac{Y_B}{R_B^3} \chi_n \right. \right\rangle_{el} Z_B \quad (49b)$$

where the many-electron operator  $Z_B/R_B^3$  refers to a coordinate system centered on the nucleus B. for  $\sigma-\sigma$  transitions,  $N_{C_2} = 0$  and for  $\sigma-\pi$  transitions  $M_{C_2} = 0$ . The computational effort is thus directed to the evaluation of the matrix elements appearing in Eqs. (49). Upon expansion of the many-electron operators, such as  $Z_B/R_B^3$ , with respect to the center of mass of the nuclei, the long-range interactions that appear in the more qualitative theories of dissociative-recombination and autoionization (Refs. 54 and 55) are recovered.

## DISCUSSION OF RESULTS

The theoretical research conducted under this program was concerned with the calculation of the dissociative-recombination reaction of electron attachment to the nitric oxide molecular ion and, in particular, to the determination of the dissociation products of this reaction. An important part of this study was the determination of accurate wavefunctions and potential energy curves for selected electronic states of the nitric oxide molecule and the evaluation of product state branching using a quantum mechanical close-coupling collision code. A second area of research involved a preliminary investigation of the most probable reaction pathway for the ion-molecule reaction  $O^+ + N_2 \rightarrow NO^+ + N$ .

### Dissociative-Recombination in $NO^+$

A theoretical research program was undertaken and directed toward the study of the kinetics of low-energy, electron-molecular, ion collision processes. This program was primarily concerned with the theoretical determination of the branching ratio for  $e + NO^+ \rightarrow N[{}^2D, {}^4S] + O[{}^3P]$ .

The first step in this research program was the accurate determination of the electronic states of NO which could represent possible dissociation channels for the reaction. Symmetry considerations dictate that the electronic states,  ${}^2\Sigma^+$ ,  ${}^2\Pi$ ,  ${}^2\Delta$ ,  ${}^2\Phi$ , are the most important channels. States of negative parity or of quartet multiplicity cannot connect with the initial state of  $e + NO^+$  in a first order approximation. Only spin-orbit coupling or two-electron excitation matrix elements (both of which are weak for this system) can give rise to second-order coupling. Higher electronic states have non-connecting matrix elements for the interaction potential. The method of calculation which was employed for these electronic states of NO (full CI) was capable of yielding wavefunctions which asymptotically connect to the correct atomic limits, but which indicated a smoothly varying and increasing error for shorter internuclear separations owing to nonoptimization of the inner-shell basis. This error could be analyzed quantitatively for any given molecular symmetry by comparing the calculated potential curves with the known experimental levels for the lowest state of a given symmetry. Application of these correction curves to the calculated potential curves yields a rationalized estimate of the true behavior of the excited electronic states of any given symmetry. This procedure is based on the assumption that the full CI calculations yield a correct relative picture of the excited electronic states. This implies that most of the valence shell correlation energy has been adequately described by these full CI calculations.

The results of this study of the electronic states of NO indicate that states of  $^2\Sigma^+$ ,  $^2\Pi$ , and  $^2\Delta$  symmetry will be effective in low-energy dissociative-recombination of  $e + NO^+$ . Calculations were performed for electronic states of NO in various approximations including minimum basis, double zeta and d-type polarization functions. The final adjusted energies for  $^2\Sigma^+$ ,  $^2\Pi$ , and  $^2\Delta$  symmetries of NO are shown in Fig. 1 which represents the most probable set of potential curves which lead to dissociative-recombination.

The dissociative-recombinations cross-sections are evaluated employing the direct attachment process. This direct process is governed by the matrix element  $\langle \Psi_{NO^+} | f | V(R) | \Psi_{NO} \rangle$  where  $\Psi_{NO}$  refers to the dissociating neutral molecular state of NO. Previous calculations have shown that the direct attachment process will dominate if the Franck-Condon overlap between  $NO^+$  and the dissociating channels of NO is favorable. Figure 1 indicates this to clearly be the case for this system.

The calculated rate constants as a function of the electron temperature for the dissociating channels  $^2\Sigma^+$ ,  $B^2\Pi$  II,  $^2\Pi$  III,  $^2\Delta$ , and  $^2\Phi$  are given in Tables 1 and 2. These channels are the only significant dissociation channels up to about 20,000°K. These calculated rates show a complicated behavior with vibrational quantum number of the molecular ion and tend to reinforce our previous conclusions (Ref. 58) that simple models which assume that recombination into higher vibrational states of the ion can be neglected are probably invalid. Here we find recombination into the second vibrational state occurs at a larger rate than into the ground state. The more basic parameters for this reaction are the collision cross-sections as a function of electron energy of the  $NO^+$  ion. These are presented in Table 3 for recombination into the ground vibrational state.

The summed contribution of all dissociating channels is shown in Tables 1 and 2. Only the  $^2\Sigma^+$  and  $^2\Pi$  states appear to contribute significantly to the overall recombination rate. The contribution of  $^2\Delta$  is ~ 60 percent with the remainder being primarily  $B^2\Pi$  II, at least for temperatures below ~10,000°K.

At higher energies the  $^2\Pi$  III becomes increasingly more important and, in fact, is the dominant dissociating channel above ~ 2.0 eV. This situation leads to a total recombination cross-section with some indicated structure. A comparison of these calculated data with the most recent experimental data is shown in Fig. 2.

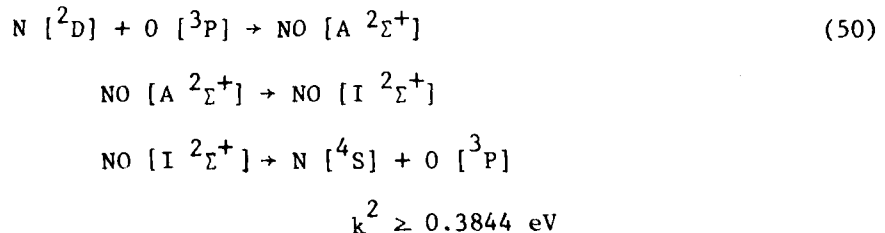
All of the primary dissociating channels lead to  $N^2D + O^3P$  atomic states as can be seen in Fig. 1. The only ambiguity is for  $^2\Sigma^+$  symmetry where an avoided crossing occurs between states I  $^2\Sigma^+$  I and A  $^2\Sigma^+$  II. The former leads to  $N^4S + O^3P$  and the latter to  $N^2D + O^3P$  if diabatic behavior is followed through the crossing point. A Landau-Zener analysis at this crossing point

indicates that the diabatic curves should be followed, but the calculation is very sensitive to the choice of the interaction energy,  $H_{ij}$ . Thus a full quantum mechanical close-coupling calculation of the branching was required for this system.

There are several approaches to the quantum theory of reactive scattering. Most of these approaches differ in their treatment of the coordinate framework for describing the collision process and in the detailed asymptotic description of reactants and products.

In the present study, we utilize the general approach of Diestler (Ref. 59) as implemented by Schmalz, Stechel, and Light (Ref. 60) for the general problem of charge transfer and exchange reactions. In this work a non-orthogonal or diabatic basis set is utilized to represent the reactant and product states. The solution of the coupled Schrödinger equations describing the nuclear motion is carried out numerically using modified R-matrix propagator techniques.

The reaction under study can be written as:



The branching ratio analysis is illustrated in Fig. 3 which indicates that for dissociative-recombination of  $e + NO^+$  into the  $A {}^2\Sigma^+$  channel, we need to consider the equivalent scattering problem shown in Eq. (50) for scattering energies  $\geq 0.3844 \text{ eV}$ , a value corresponding to zero kinetic energy attachment of an electron to  $NO^+$ .

The adiabatic potential curves for the lowest two  ${}^2\Sigma^+$  states of NO were converted to diabatic form by interpolation through the crossing region. Our calculated diabatic potential curves for  ${}^2\Sigma^+$  symmetry are given in Table 4 where we see that the maximum Hamiltonian interaction term,  $H_{ij}$ , is  $270 \text{ cm}^{-1}$  at an internuclear separation of 2.842 bohrs. The detailed shape of this diabatic interaction potential is shown in Fig. 4. The smallness of this interaction term indicates that coupling is weak between these lowest two  ${}^2\Sigma^+$  states and that diabatic collision behavior is indicated.

Detailed calculations of the cross-sections for the reaction illustrated in Eq. (50) were carried out for collision energies  $0.3844 \leq E(\text{eV}) \leq 2.00$ . This corresponds to electron attachment in the energy region  $0 \leq E(\text{eV}) \leq 1.6 \text{ eV}$ . Our calculated collision cross-sections are shown in Table 5 where we see that the coupling cross-section between  $\text{I } ^2\Sigma^+$  and  $\text{A } ^2\Sigma^+$  of NO never exceeds  $\sigma \sim 1 \times 10^{-5} a_0^2 (3 \times 10^{-22} \text{ cm}^2)$ . We are thus led to the prediction that the recombination along the  $\text{A } ^2\Sigma^+$  channel follows a diabatic reaction path and we predict exclusively that  $\text{N}(^2\text{D}) + \text{O}(^3\text{P})$  are the atomic products of dissociative-recombination of  $e + \text{NO}^+$ .

#### Comparison With Experimental Data

The calculated data show a low-temperature variation as  $T_e^{-0.39}$  for  $v = 0$  and  $T_e^{-0.47}$  for  $v = 2$ , a result which is not in accord with the results obtained in a microwave-afterglow-mass-spectrometer by Gunton and Shaw (Ref. 61) but is in excellent agreement with the experimental data of Huang, Biondi and Johnson (Ref. 62). This agreement may be somewhat fortuitous since Huang, et al. almost certainly measured recombination primarily into the second vibrational level of  $\text{NO}^+$ . Our predicted temperature dependence of the rate coefficient for  $v = 2$  is in somewhat poorer agreement with their experiments.

Another feature of the comparison with the data of Huang, et al. is the indicated strong increase in the recombination rate at temperature  $< 300^\circ\text{F}$ . This may be due to secondary attachment processes (recombination into vibrationally excited Rydberg states of NO) which will become more important at lower electron temperatures (Ref. 63). The overall rates are in numerical agreement within our calculation uncertainty.

The recent ion recombination studies by Walls and Dunn (Ref. 64) show a stronger energy dependence in the measured cross-sections than that found theoretically from these studies for electron temperatures below about 0.1 eV. Examination of Fig. 5 shows that the cross-section should approach  $1/e$  behavior at about 0.04 eV whereas the data of Walls and Dunn clearly exhibit a different energy dependence in this region. The major problem seems to be the experimental data point at  $\sim 0.04 \text{ eV}$ . A recent reexamination of these data by Walls and Dunn (Ref. 65) indicate a large experimental uncertainty at these very low electron energies; their lower uncertainty nearly bracketing our calculated data. The inferred recombination rates from the data of Walls and Dunn show a very strong temperature dependence ( $T_e^{-0.83}$ ) arising from the low energy dependence of their measured cross-section data.

The agreement between calculated and measured cross-sections above 0.1 eV is excellent even to systematics in the structure which arise from a changing importance of the dissociating channels as a function of increasing electron energy. The flattening of the cross-section above  $\sim 1.5 \text{ eV}$  is the result of

competing effects between the  $B^2\Pi$  II and  $A^2\Pi$  III dissociating channels. The latter is becoming more important in this energy region and shows a weaker energy dependence, hence a leveling off effect occurs in the total cross-section. This qualitative agreement tends to verify that we are considering the correct molecular states of NO as the dissociating channels.

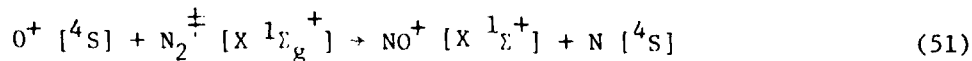
The data of Gunton and Shaw (Ref. 61) are suspect owing to dimer ion effects. The importance of ion clustering at low temperatures is uncertain for the other experiments.

A further question is the importance of autoionization, which may be enhanced at the lower energies for this reaction. A crude calculation of the survival factor as defined by Bardsley (Ref. 49) indicates that it should be close to unity. Further detailed studies are required for a more quantitative analysis of the role of autoionization at the lower electron energies.

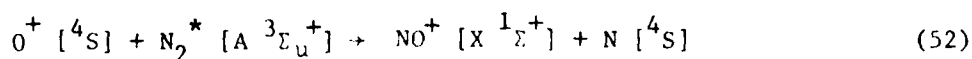
Our calculated rate coefficients may be considered to be valid only up to about 10,000°K. Above this temperature, our analysis is incomplete owing to increased population of the higher vibrational structure and the neglect of other electronic states. The comparison with the high-temperature data of Stein (Ref. 66) and Lin and Tease (Ref. 65) appear to indicate a much stronger electron-temperature dependence than that found in these calculations or that can even be inferred from the data of Walls and Dunn.

#### O<sup>+</sup> + N<sub>2</sub> Ion-Molecule Reaction

As a continuation of our theoretical research on atmospheric chemistry, we undertook a preliminary examination of the reaction kinetics and branching ratios for the ion-molecule reaction  $O^+ + N_2 \rightarrow NO^+ + N$ . The particular reactions which are most important in NO<sup>+</sup> formation are:



$$\Delta E = + 1.1 \text{ eV}$$

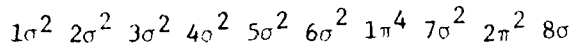


$$\Delta E = + 7.3 \text{ eV}$$

The molecular correlations which connect reactant to product states are uncertain. A complete  $N_2O^+$  correlation diagram is shown in Table 6 which lists the reactant and product states in increasing energy without symmetry considerations. The lowest quartet state in a linear ( $C_{\infty v}$ ) O-N<sub>2</sub><sup>+</sup> configuration corresponds to  ${}^4\Sigma^-$  symmetry. In a bent ( $C_s$ ) geometry, this lowest

configuration belongs to  $^4A''$ . Hopper (Ref. 68) has carried out SCF calculations for several symmetries of  $N_2O^+$  and has suggested a complicated reaction pathway in which  $O^+ + N_2$  first combine in a linear configuration and then form a bent conformation with  $N [^4S]$  finally leaving at  $90^\circ$  relative to the original collision. Hopper calculates the lowest saddle point in the collinear  $^4\Sigma^-$  symmetry to be at least 7 eV above the  $O^+ [^4S] + N_2 [^1\Sigma_g^+]$  asymptote. This is energetically inaccessible for low-energy  $O^+ + N_2$  collisions and thus he favors the distorted reaction path in  $C_s$  symmetry.

Previous studies in this Center (Ref. 69) on  $NO_2^+$  have shown that SCF or MCSCF calculations may exhibit artificially high reaction barriers in  $C_{\infty v}$  symmetry. The origin of the problem is that SCF or MCSCF methods generally employ maximum pairing in their MO structure. The SCF structure of  $N_2O^+ [^4\Sigma^-]$  can be written as:



where at short  $O^+ - N_2$  separations we can identify the principal AO composition of these MO's as follows:

$$\begin{aligned} 1\sigma, \ 2\sigma, \ 3\sigma &= 1s \\ 4\sigma &= 2s_O \\ 5\sigma &= 2s_N \text{ (outer)} \\ 6\sigma &= 2s_N \text{ (inner)} \\ 7\sigma &= 2p\sigma \text{ (NO)} \\ 8\sigma &= 2p\sigma_N \text{ (outer)} \\ 9\sigma &= 2p\sigma^* \text{ (NO)} \\ 1\pi &= 2p\pi \text{ (NO)} \\ 2\pi &= 2p\pi_N \text{ (inner)} \\ 3\pi &= 2p\pi \text{ (NO)} \end{aligned}$$

At large  $O^+ - N_2$  separations, the MO composition for the 2p electrons must be:

$$\begin{aligned} 7\sigma &= 2p\sigma \text{ (N}_2\text{)} \\ 8\sigma &= 2p\sigma \text{ (O}^+\text{)} \\ 1\pi &= 2p\pi \text{ (N}_2\text{)} \\ 2\pi &= 2p\pi \text{ (O}^+\text{)} \end{aligned}$$

Thus both the  $\sigma$  and  $\pi$  orbitals are completely recoupled spin-wise in going from  $O^+ + N_2$  to  $N + NO^+$ . In Fig. 6 we present a general vector coupling diagram which indicates that there are 48 separate spin-states for nine electron quartet coupling. Reactions (51) and (52) involve a complete spin-recoupling as the pairing changes in going from reactants to products which suggests that a valence bond treatment is more appropriate than SCF or limited MCSCF expansions. Previous studies on the much simpler  $H_3$  surface have indicated the importance of including higher spin-coupled states (Ref. 70).

Our preliminary studies indicate that the spin-recoupling that occurs in going from reactants to products is not adequately represented within SCF or MCSCF frameworks. A calculation for  $^4\Sigma^-$  of  $N_2O^+$  at intermediate internuclear separations yields a spin-correlation error of 6 eV. This value closely corresponds to the 7 eV barrier found in the MCSCF calculations by Hopper. We propose to examine the lowest energy  $^4\Sigma^-$  potential energy surface of  $N_2O^+$  within an ab-initio CI framework including all possible spin and spatial projections of the 2p electrons. Based on our previous studies of  $H_3$  and  $NO_2$ , we believe that a linear pathway of much lower energy than that predicted from SCF calculations will be found. A schematic of our predicted reaction pathway is illustrated in Fig. 7. A similar analysis will be carried out for  $O^+({}^4S) + N_2^* (A {}^3\Sigma_u^+)$ , where both doublet and quartet channels will be examined.

## REFERENCES

1. Harang, O.: A10 Resonant Spectrum for Upper Atmosphere Temperature Determination. AFCRL-66-314, Environmental Research Paper, No. 192, 1966.
2. Churchill, D. R. and R. E. Meyerott: "Spectral Absorption in Heated Air," Journal of Quantitative Spectroscopy and Radiative Transfer, Vol. 5, p. 69, 1965.
3. The Airglow and the Aurorae, edited by E. B. Armstrong and A. Dalgarno. Pergamon Press, New York, 1955.
4. Armstrong, B. H., R. R. Johnston and P. S. Kelly: "The Atomic Line Contribution to the Radiation Absorption Coefficient of Air," Journal of Quantitative Spectroscopy and Radiative Transfer, Vol. 5, pp. 55, 1965.
5. Johnston, R. R., B. H. Armstrong and O. R. Platas: "The Photoionization Contribution to the Radiation Absorption Coefficient of Air," Journal of Quantitative Spectroscopy and Radiative Transfer, Vol. 5, p. 49, 1965.
6. Harris, F. E. and H. H. Michels: "Open-Shell Valence Configuration - Interaction Studies of Diatomic and Polyatomic Molecules," International Journal of Quantum Chemistry, Vol. IS, p. 329, 1967.
7. Krauss, M.: Compendium of ab initio Calculations of Molecular Energies and Properties. NBS Technical Note 438, December 1967.
8. Wahl, A. C., P. J. Bertoncini, G. Das and T. L. Gilbert: "Recent Progress Beyond the Hartree-Fock Method for Diatomic Molecules. The Method of Optimized Valence Configurations," International Journal of Quantum Chemistry, Vol. IS, p. 123, 1967.
9. Schaefer, H. F.: Electronic Structure of Atoms and Molecules, Addison-Wesley Publishing Co., 1972.
10. Neynaber, R. H. and G. D. Magnuson: "Low Energy Study of  $O + N_2 \rightarrow NO^+ + N$ ," Journal of Chemical Physics, Vol. 58, p. 4586, 1973.
11. Allen, L. C.: Quantum Theory of Atoms, Molecules and the Solid State, Edited by P. O. Lowdin, Academic Press, Inc., New York.

REFERENCES (Cont'd)

12. Roothan, C. C. J. and P. S. Bagus: "Atomic Self-Consistent Field Calculations by the Expansion Method," Methods in Computational Physics, Edited by B. Alder, Vol. 2, p. 47, 1963.
13. Roothan, C. C. J.: "New Developments in Molecular Orbital Theory," Reviews of Modern Physics, Vol. 23, No. 2, April 1951, p. 69.
14. Harris, F. E.: "Molecular Orbital Studies of Diatomic Molecules. I. Method of Computation for Single Configurations of Heteronuclear Systems," Journal of Chemical Physics, Vol. 32, p. 3, 1960.
15. Harris, F. E.: "Open-Shell Orthogonal Molecular Orbital Theory," Journal of Chemical Physics, Vol. 46, p. 2769, 1967.
16. Givens, W.: Eigenvalue-Eigenvector Techniques, Oak Ridge Report Number ORNL 1574 (Physics).
17. Shavitt, I., C. F. Bender, A. Pipano, and R. P. Hosteny: "The Iterative Calculation of Several of the Lowest or Highest Eigenvalues and Corresponding Eigenvectors of Very Large Symmetric Matrices," Journal of Computational Physics, 11, p. 90, 1973.
18. Schaefer, F. E. and F. E. Harris: "Ab Initio Calculations of 62 Low-Lying States of the O<sub>2</sub> Molecule," Journal of Chemical Physics, Vol. 8, p. 4946, 1968.
19. Michels, H. H. and F. E. Harris: "Predissociation Effects in the A <sup>2</sup> $\Sigma^+$  State of the OH Radical," Chemical Physics Letters, Vol. 3, p. 441, 1969.
20. Harris, F. E. and H. H. Michels: "The Evaluation of Molecular Integrals for Slater-Type Orbitals," Advances in Chemical Physics, Vol. 13, p. 205, 1967.
21. Davidson, E. R.: "Natural Expansions of Exact Wavefunctions, III. The Helium Atom Ground State," Journal of Chemical Physics, Vol. 39, p. 875, 1963.
22. Aaron, R., R. Amado and B. Lee: "Divergence of the Green's Function Series for Rearrangement Collisions," Phys. Rev., Vol. 121, p. 319, 1961.

REFERENCES (Cont'd)

23. Bates, D. R. and R. McCarroll: "Charge Transfer," Suppl. Phil. (Advances in Physics), Vol. 11, p. 39, 1962.
24. Bates, D. R. and R. McCarroll: "Electron Capture in Slow Collisions," Proc. Roy. Soc. (London), Vol. A245, p. 175, 1958.
25. Bates, D. R. and D. A. Williams: "Low-Energy Collisions Between Hydrogen Atoms and Protons," Proc. Phy. Soc., Vol. A83, p. 425, 1964.
26. Fulton, M. J. and M. H. Mittlemen: "Scattering of  $H^+$  by H," Annals of Physics, Vol. 33, pp. 65-76, 1965.
27. Quong, J.: Approximations in the Theory of Rearrangement Collisions and Applications to a Tractable Model of Charge-Exchange Scattering, Lawrence Radiation Laboratory Report UCRL-17034, August 19, 1966.
28. Riley, M. E.: "Strong-Coupling Semiclassical Methods. The Average Approximation for Atom-Atom Collisions," Phy. Rev. A, Vol. 8, p. 742, 1973.
29. Massey, H. S. W. and R. A. Smith: Proc. Roy. Soc. (London), Vol. A126, p. 259, 1930.
30. Dalgarno, A. and R. McCarroll: "Adiabatic Coupling Between Electronic and Nuclear Motion in Molecules," Proc. Roy. Soc., Vol. A237, p. 383, 1956.
31. Hahn, Y.: "Distorted Cluster States in Scattering Theory," Phys. Rev., Vol. 154, p. 981, 1967.
32. Marchi, R. P. and F. T. Smith: "Theory of Elastic Differential Scattering in Low-Energy  $He^+ + He$  Collisions," Phys. Rev., Vol. 139, p. A1025, 1965.
33. Smith, F. J.: "The Probability of Electron Capture at Fixed Scattering Angles in  $H^+ - H$  Collisions," Proc. Phy. Soc., Vol. 84, p. 889, 1964.
34. Dalgarno, A.: "Spin-Exchange Cross Sections," Proc. Roy. Soc., Vol. 262A, p. 132, 1961.
35. Kolker, H. J. and H. H. Michels: "Elastic Scattering, Diffusion and Excitation Transfer of Metastable Helium in Helium," J. Chem. Phys., Vol. 50, p. 1762, 1969.

REFERENCES (Cont'd)

36. Harris, F. E.: "Molecular Orbital Studies of Diatomic Molecules. I. Method of Computation for Single Configurations of Heteronuclear Systems," J. Chem. Phys., Vol. 32, p. 3, 1960.
37. Schneiderman, S. B. and H. H. Michels: "Quantum-Mechanical Studies of Several Helium-Lithium Interaction Potentials," J. Chem. Phys., Vol. 42, p. 3706, 1966.
38. Michels, H. H.: "Molecular Orbital Studies of the Ground and Low-Lying Excited States of the  $\text{HeH}^+$  Moelcular Ion," J. Chem. Phys., Vol. 44, p. 3834, 1966.
39. Schneiderman, S. B. and A. Russek: "Velocity-Dependent Orbitals in Proton-On-Hydrogen Atom Collisions," Phys. Rev., Vol. 181, p. 311, 1969.
40. Thorson, W. R.: "Theory of Slow Atomic Collisions I.  $\text{H}_2^+$ ," J. Chem. Phys., Vol. 42, p. 3878, 1965.
41. Kouri, D. J. and C. F. Curtiss: "Phase Shifts and the Quantum-Mechanical Hamilton-Jacobi Equation," J. Chem. Phys., Vol. 43, p. 1919, 1965.
42. Zemach, C.: "Phase-Shift Equations for Many Channel Problems," Nuovo Cimento, Vol. 33, p. 939, 1964.
43. Kouri, D. J. and C. F. Curtiss: "Low-Energy Atomic Collisions I. The Schrödinger Equation for  $\text{H}^+-\text{H}$ ," J. Chem. Phys., Vol. 44, p. 2120, 1966.
44. Mittleman, M. H.: "Proton-Hydrogen Scattering System," Phys. Rev., Vol. 122, p. 499, 1961.
45. Bates, D. R. and A. R. Holt: "Impact Parameter and Semiclassical Treatments of Atomic Collisions," Proc. Phy. Soc., Vol. 85, p. 691, 1965.
46. Stückelberg, E. C. G.: Helv. Phys. Acta, Vol. 5, p. 369, 1932.
47. Russek, A.: "Rotationally Induced Transition in Atomic Collisions," Physical Review A, Vol. 4, p. 1918, 1971.

## REFERENCES

48. Bates, D.R.: "Dissociative Recombination," Physical Review, Vol. 78, 1959, p. 492.
49. Bardsley, J.N.: "The Theory of Dissociative Recombination," Proceedings of the Physical Society, Vol. 1B, 1968, p. 365.
50. Berry, R.S. and S.E. Nielson: "Dynamic Coupling Phenomena in Molecular Excited States. I: Formulation and Vibronic Coupling in H<sub>2</sub>," Physical Review, Vol. 1-A, 1970, p. 383.
51. Berry, R.S. and S.E. Nielson: "Dynamic Coupling Phenomena in Molecular Excited States. II: Autoionization and Predissociation in H<sub>2</sub>, HD, and D<sub>2</sub>," Physical Review, Vol. 1-A, 1970, p. 395.
52. Cook, G.R. and P.H. Metzger: "Photoionization and Absorption Cross Sections of O<sub>2</sub> and N<sub>2</sub> in the 600- to 1000-A Region," Journal of Chemical Physics, Vol. 41, 1964, p. 321.
53. Nielson, S.E. and J.S. Dahler: "Theory of the Dissociation Recombinations and Associative Ionization of Hydrogen," Journal of Chemical Physics, Vol. 45, 1964, p. 4060.
54. Russek, A., M.R. Patterson and R.L. Becker: "Auto-Ionization in Molecular Systems," Physical Review, Vol. 167, 1968, p. 17.
55. Bardsley, J.N.: "The Ionization of Molecules Near Threshold," Chemical Physics Letters, Vol. 1, 1967, p. 229.
56. Nielson, S.E. and R.S. Berry: "Vibronic Autoionization and Predissociation in Hydrogen," Chemical Physics Letters, Vol. 2, 1968, p. 503.
57. Bates, D.R., H.S.N. Massey and A.L. Stewart: "Inelastic Collisions Between Atoms. I: General Theoretical Considerations," Proceedings of the Royal Society, Vol. 216A, 1953, p. 437.
58. Michels, H. H.: "Theoretical Determination of Electronic Transition Probabilities for Diatomic Molecules", Final Technical Report No. AFWL-TR-72-1, Kirtland Air Force Base, New Mexico, May 1972.
59. Diestler, D. J.: "Close-Coupling Technique for Chemical Exchange Reaction of the type A + BC → AB + C, H + H<sub>2</sub> → H<sub>2</sub> + H<sup>\*</sup>," Journal of Chemical Physics, Vol. 54, 1971, p. 4547.

REFERENCES (Cont'd)

60. Schmalz, T. G., E. B. Stechel, and J. C. Light: "Time Independent Quantum Theory of Electron Transfer Collision Using a Non-Orthogonal Basis and R-Matrix Propagation," Journal of Chemical Physics, Vol. 70, 1979, p. 5660.
61. Gunton, R. C. and T. M. Shaw: "Electron-Ion Recombination in Nitric Oxide in the Temperature Range 196 to 358°K," Physical Review, Vol. 140A, 1965, p. 756.
62. Huang, C. M., M. A. Biondi, and R. Johnsen: "Variation of Electron-NO<sup>+</sup>-ion Recombination Coefficient with Electron Temperature," Physical Review, Vol. 11A, 1975, p. 901.
63. Bardsley, J. N.: Private Communication
64. Walls, F. L. and G. H. Dunn: "Measurement of Total Cross Section for Electron Recombinations with NO<sup>+</sup> and O<sub>2</sub><sup>+</sup> Using Ion Storage Techniques," Journal of Geophysical Research, Vol. 79, 1974, p. 1911.
65. Walls, F. L. and G. H. Dunn: Private Communication.
66. Stein, R. P., M. Scheibe, M. W. Syverson, T. M. Shaw and R. C. Gunton: "Recombination Coefficient of Electrons with NO<sup>+</sup> Ions in Shock-Heated Air," Physics of Fluids, Vol. 7, 1964, p. 1641.
67. Lin, S. C. and J. D. Tease: "Rate of Ionization Behind Shock Waves in Air, II. Theoretical Interpretations", Physics of Fluids, Vol. 6, 1963, p. 355.
68. Hopper, D. G.: "Mechanisms of the Reaction of Positive Atomic Oxygen Ions with Nitrogen", Journal of the American Chemical Society, Vol. 100, 1978, p. 1019.
69. Michels, H. H.: "Theoretical Research Investigation Upon Reaction Rates Relating to the Nitric Oxide (Positive) Ion", UTRC Progress Report R79-922102-9, November 15, 1979, United Technologies Research Center.
70. Michels, H. H. and F. E. Harris: "Configuration-Interaction Study of The Linear H<sub>3</sub> System", Journal of Chemical Physics, Vol. 48, 1968, p. 2371.

REFERENCES (Cont'd)

71. Rutherford, J. A., R. H. Neynaber and D. A. Vroom: "Measurements of Selected Charge Transfer Processes at Low Energies," IRT Corporation Final Report (IRT 8163-007) Defense Nuclear Agency Report No. DNA 4695F, 1978.

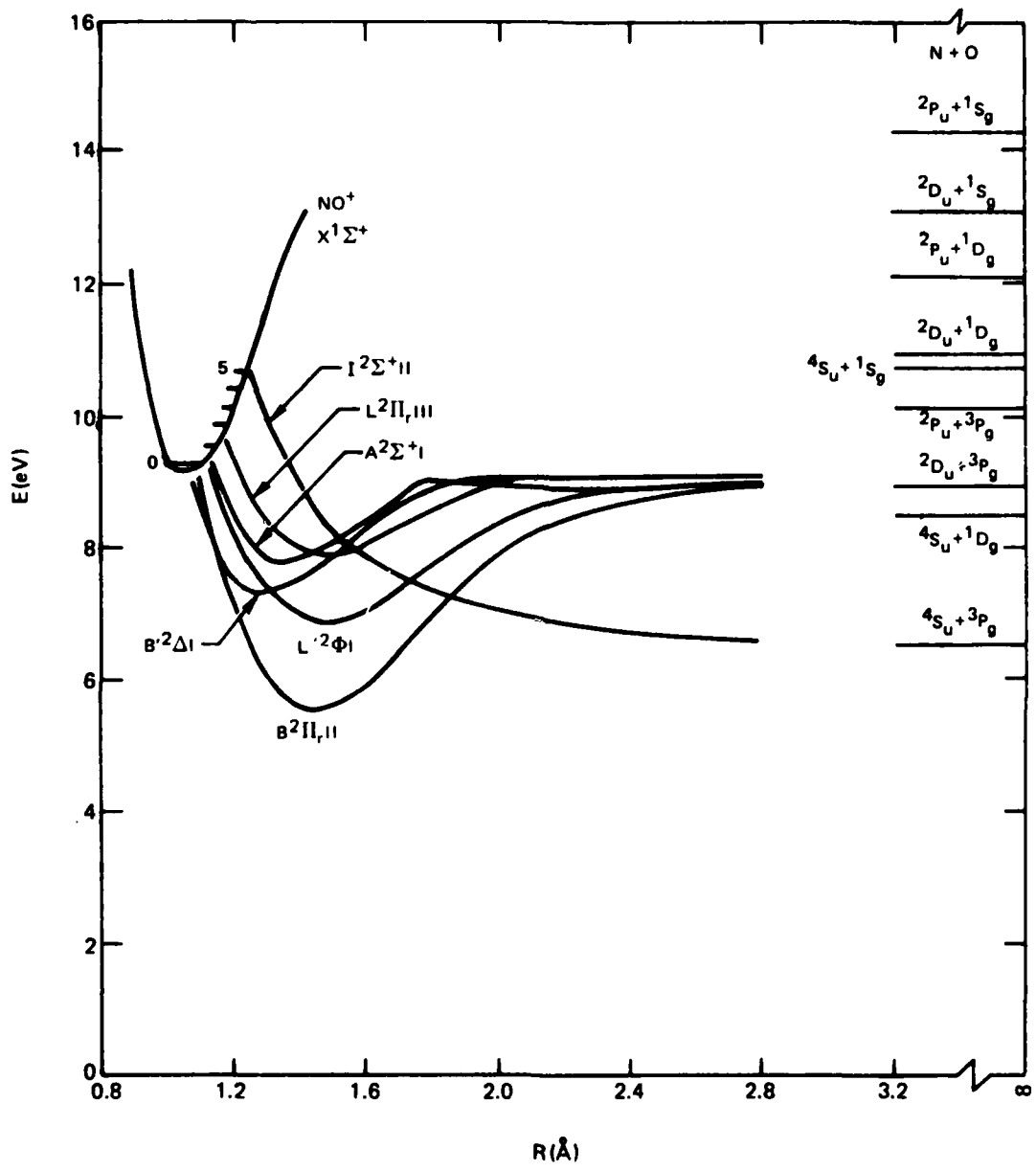


**Figure 1 Potential Energy Curves of NO Leading to Dissociative Recombination in  $\text{NO}^+$**

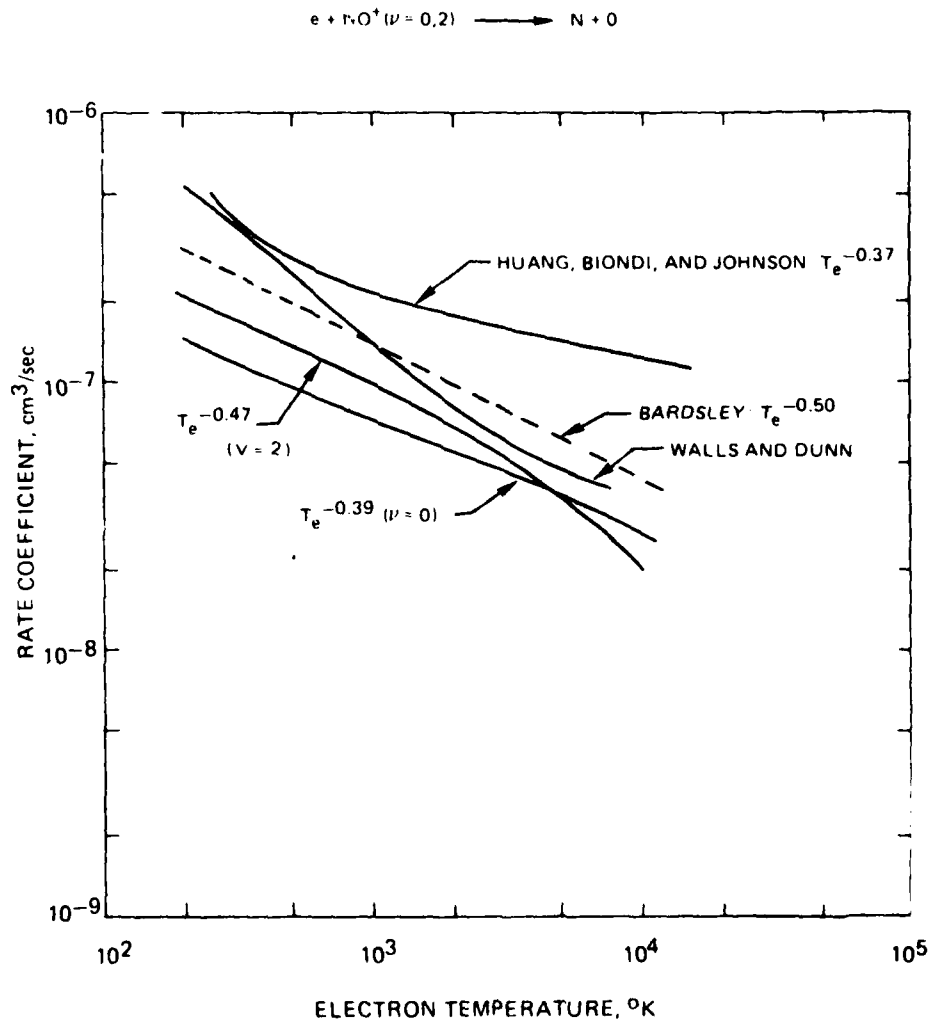
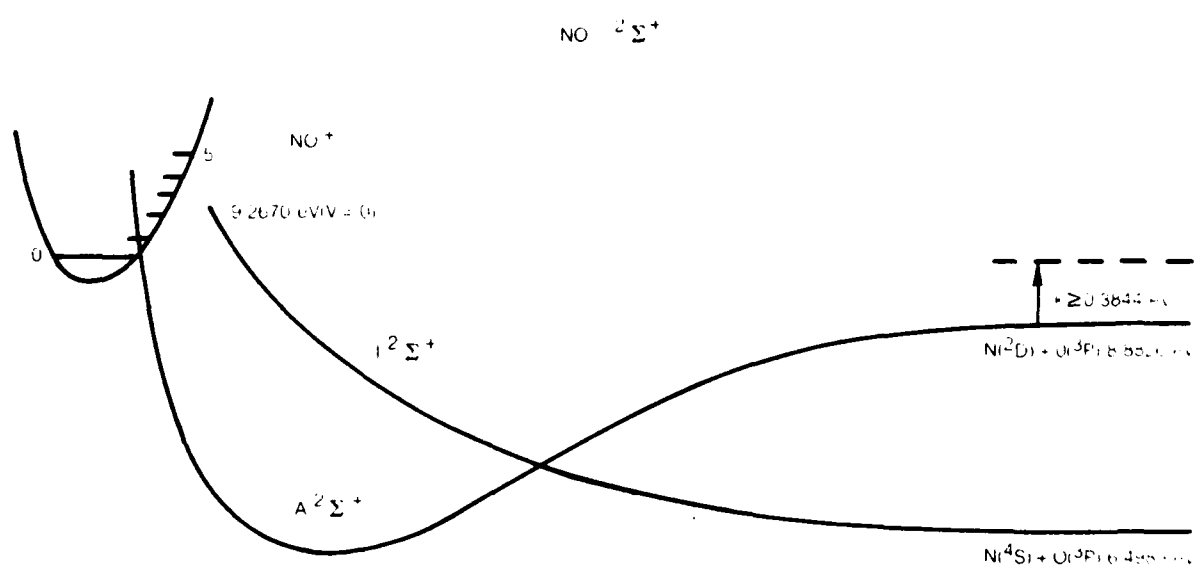
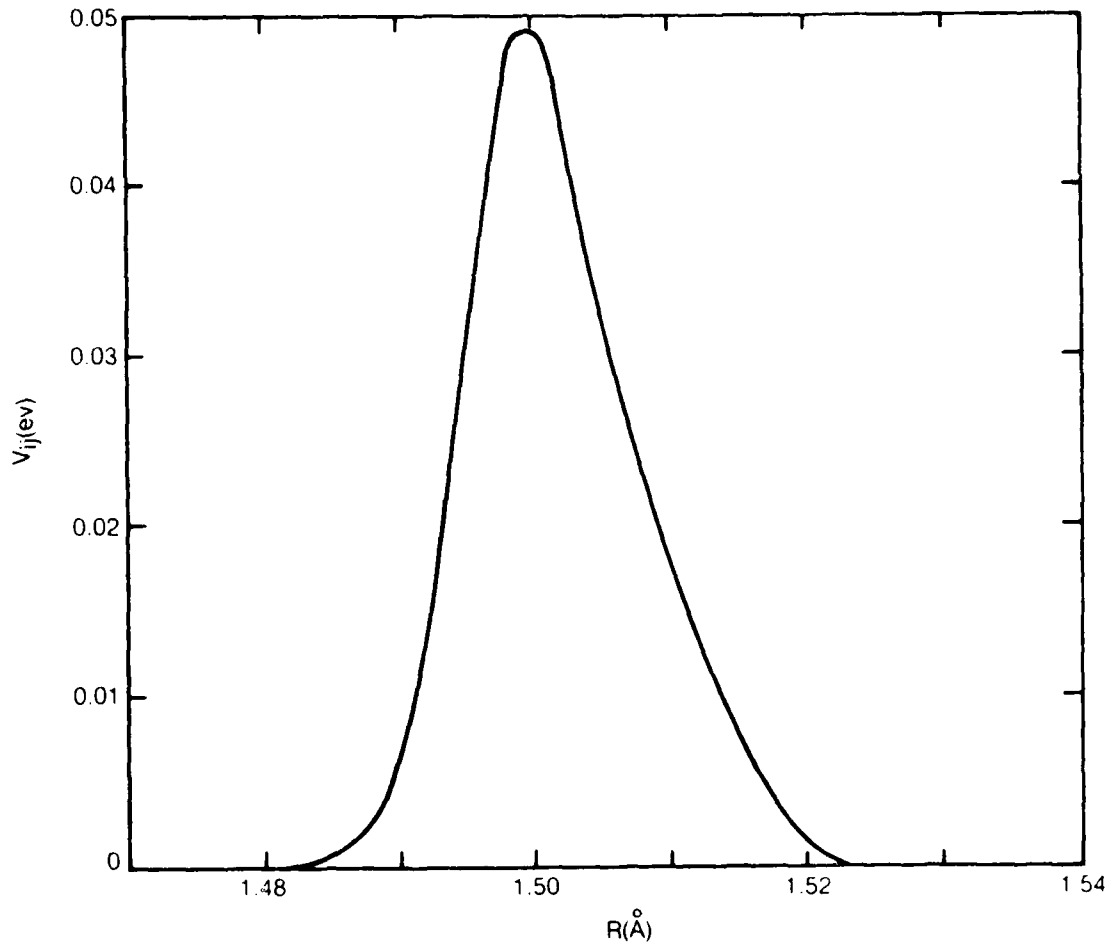


FIGURE 2. DISSOCIATIVE RECOMBINATION RATE COEFFICIENT,  $\text{cm}^3/\text{SEC}$



**Figure 3 Branching Ratio Analysis**



**Figure 4 Interaction Potential for NO ( $A\ 2\Sigma^+ - 1\Sigma^+$ )**

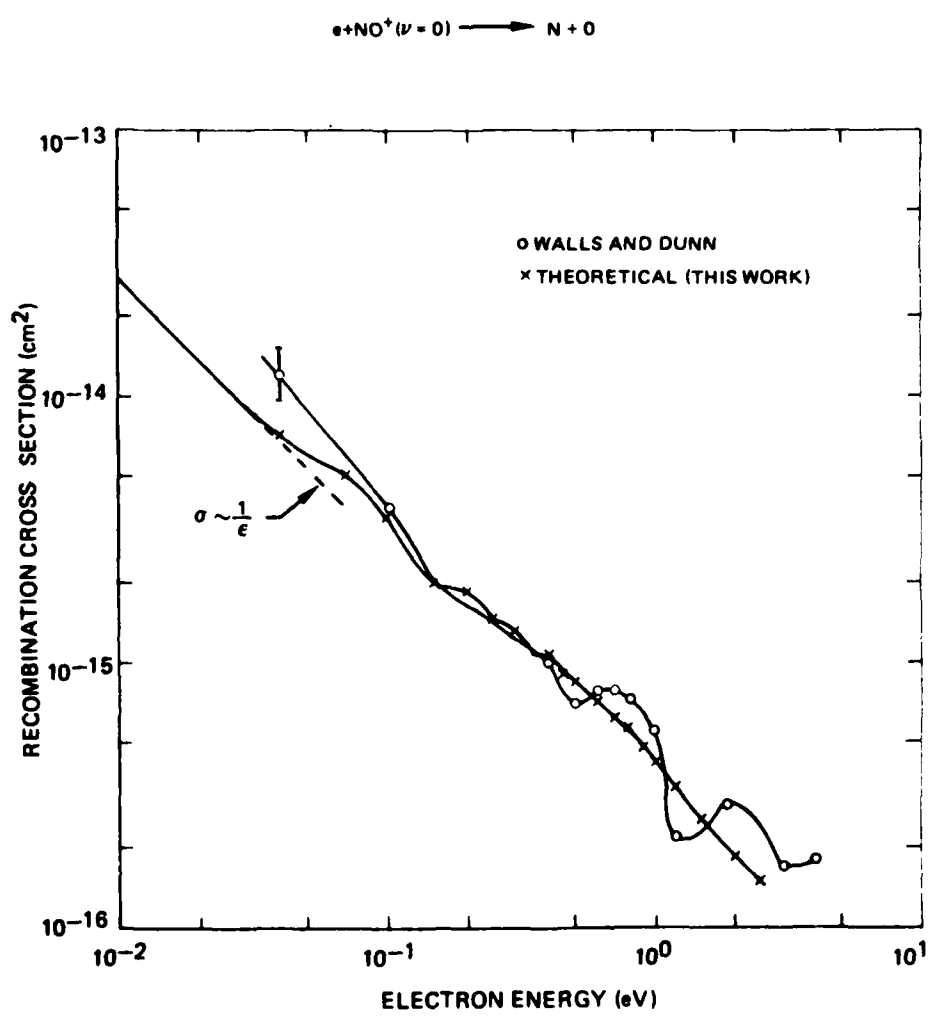


FIGURE 5. TOTAL RECOMBINATION CROSS SECTION,  $\text{cm}^2$

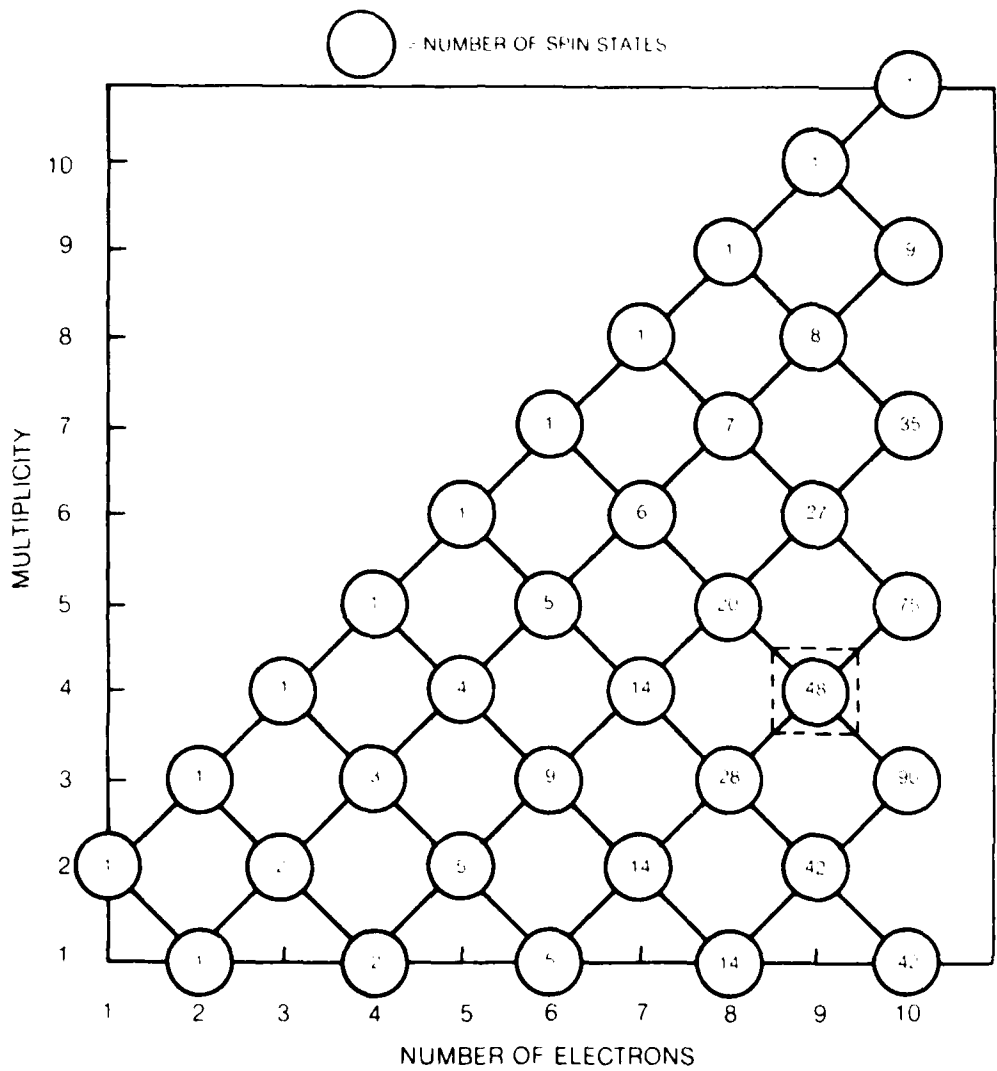


Figure 6 Vector Coupling Diagram For Electron Spin

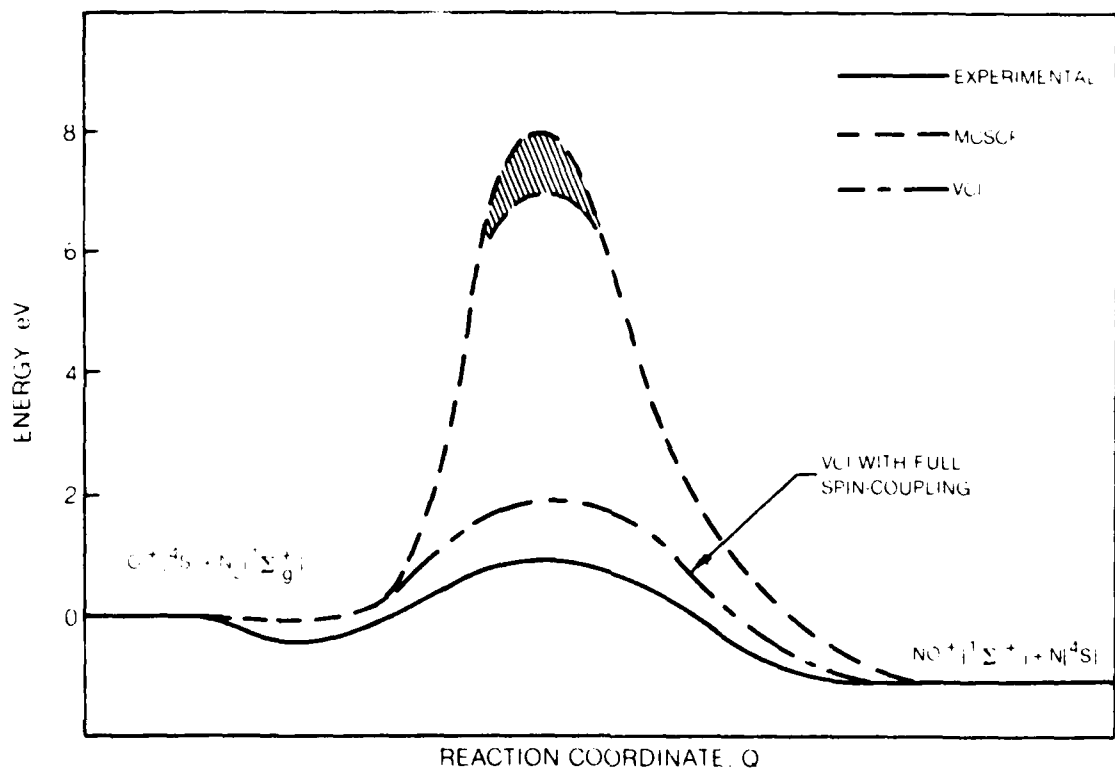
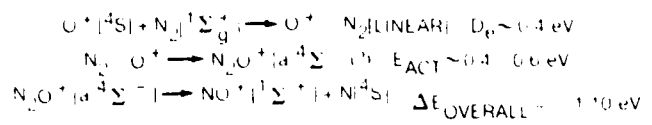


Figure 7 Co-Linear Reaction Pathway for  $\text{O}^+ + \text{N}_2$

TABLE 1  
CALCULATED DISSOCIATIVE-RECOMBINATION RATE COEFFICIENTS

T °K	$\alpha (T_e, v = 0), \text{ cm}^3/\text{sec}$					
	$\alpha_{2\Sigma^+}$	$\alpha_B 2\Pi$	$\alpha^2\Pi_{\text{III}}$	$\alpha_{B'} 2\Delta$	$\alpha^2\Phi$	$\alpha_{\text{Total}}$
200	9.216-08	4.437-08	1.615-09	4.423-09	1.342-10	1.427-07
298.16	7.806-08	3.669-08	1.366-09	3.614-09	1.122-10	1.198.07
400	6.960-08	3.194-08	1.221-09	3.114-09	9.895-11	1.060-07
600	5.969-08	2.640-08	1.071-09	2.538-09	8.420-11	8.978-08
800	5.348-08	2.310-08	9.975-10	2.195-09	7.599-11	7.985-08
1000	4.918-08	2.085-08	9.610-10	1.962-09	7.090-11	7.302-08
2000	3.811-08	1.526-08	9.888-10	1.377-09	6.324-11	5.580-08
4000	2.903-08	1.122-08	1.416-09	9.256-10	7.218-11	4.266-08
6000	2.347-08	9.167-09	2.027-09	6.993-10	8.009-11	3.544-08
8000	2.020-08	7.919-09	2.581-09	5.502-10	8.113-11	3.133-08
10000	1.715-08	6.892-09	2.970-09	4.517-10	7.792-11	2.754-08

TABLE 2  
CALCULATED DISSOCIATIVE-RECOMBINATION RATE COEFFICIENTS

T °K	$\alpha$ ( $T_e$ , $v = 2$ ), $\text{cm}^3/\text{sec}$						$\alpha$ Total
	$\alpha_{\Sigma^+}^2$	$\alpha_{B\Pi}^2$	$\alpha_{\Pi\text{ III}}^2$	$\alpha_{B'\Delta}^2$	$\alpha_{\Phi}^2$		
200	6.461-08	1.527-08	1.288-07	1.498-09	1.137-10		2.103-07
298.16	5.406-08	1.277-08	1.057-07	1.194-09	8.781-11		1.738-07
400	4.761-08	1.125-08	9.153-08	1.002-09	7.134-11		1.515-07
600	4.009-08	9.517-09	7.506-08	7.725-10	5.190-11		1.255-07
800	3.549-08	8.517-09	6.510-08	6.307-10	4.050-11		1.098-07
1000	3.223-08	7.853-09	5.813-08	5.319-10	3.329-11		9.878-08
2000	2.307-08	6.255-09	3.937-08	2.923-10	2.316-11		6.901-08
4000	1.470-08	4.973-09	2.394-08	1.749-10	2.877-11		4.382-08
6000	1.051-08	4.159-09	1.680-08	1.520-10	3.249-11		3.166-08
8000	8.494-09	3.539-09	1.288-08	1.422-10	3.364-11		2.509-08
10000	6.964-09	3.041-09	1.034-08	1.334-10	3.354-11		2.051-08

TABLE 3  
CALCULATED CROSS-SECTION FOR DISSOCIATIVE-RECOMBINATION,  $\text{cm}^2$

$\xi$	$e + \text{NO}^+ (\nu = 0) \rightarrow \text{N} + \text{O}$					$\sigma_{\text{Total}}$
	$\sigma_{2\Sigma^+}$	$\sigma_{B^2\Pi}$	$\sigma_{2\Pi_{\text{III}}}$	$\sigma_{B'2\Delta}$	$\sigma_{2\Phi}$	
.01	1.758-14	8.603-15	3.092-16	8.721-16	2.586-17	2.739-14
.04	4.599-15	2.260-15	8.454-17	2.146-16	6.934-18	7.165-15
.07	3.669-15	1.326-15	5.498-17	1.204-16	4.269-18	5.175-15
.10	2.537-15	9.219-16	4.276-17	8.545-17	3.170-18	3.590-15
.15	1.367-15	6.185-16	3.414-17	5.849-17	2.340-18	2.081-15
.20	1.302-15	4.990-16	2.977-17	4.280-17	1.929-18	1.875-15
.25	1.032-15	3.888-16	2.774-17	3.442-17	1.710-18	1.484-15
.30	9.440-16	3.372-16	2.690-17	2.874-17	1.568-18	1.338-15
.35	7.302-16	3.006-16	2.711-17	2.410-17	1.465-18	1.083-15
.40	7.774-16	2.558-16	2.659-17	2.114-17	1.417-18	1.082-15
.45	6.236-16	2.376-16	2.685-17	1.860-17	1.403-18	9.080-16
.50	5.899-16	2.150-16	2.694-17	1.639-17	1.409-18	8.496-16
.60	4.802-16	1.810-16	2.814-17	1.333-17	1.419-18	7.042-16
.70	4.328-16	1.499-16	3.216-17	1.086-17	1.497-18	6.272-16
.80	3.943-16	1.322-16	3.500-17	8.968-18	1.573-18	5.721-16
.90	3.235-16	1.181-16	3.741-17	7.279-18	1.721-18	4.880-16
1.00	2.777-16	1.021-16	3.785-17	5.872-18	1.946-18	4.255-16
1.20	2.118-16	8.498-17	3.968-17	3.514-18	2.461-18	3.425-16
1.50	1.357-16	6.356-17	5.104-17	1.428-18	2.005-18	2.537-16
2.00	6.601-17	3.983-17	8.066-17	3.073-19	7.722-19	1.876-16
2.50	3.234-17	2.612-17	9.338-17	6.890-20	1.828-19	1.521-16

TABLE 4

DIABATIC  $^2\Sigma^+$  POTENTIAL ENERGY CURVES FOR NO

<u>R(bohrs)</u>	<u>A <math>^2\Sigma^+</math>(a.u.)</u>	<u>I <math>^2\Sigma^+</math>(a.u.)</u>	<u><math>H_{ij} = \Delta H(A^2\Sigma^+ - X^2\Sigma^+)</math> (a.u.)</u>
2.8	-128.682681	-128.676266	.0002266
2.81	-128.682579	-128.677912	.0005507
2.82	-128.682566	-128.679408	.0009352
2.825	-128.682652	-128.680042	.0010807
2.83	-128.682865	-128.680535	.0011716
2.84	-128.680985	-128.683787	.0012275
2.85	-128.680987	-128.685105	.0012124
2.86	-128.680831	-128.686532	.0010722
2.9	-128.679802	-128.692210	.0000281

TABLE 5  
EXCITATION CROSS-SECTIONS FOR  $^2\Sigma^+$  STATES OF NO

Channel 11 = N [ $^2D$ ] + O [ $^3P$ ]; Channel 22 = N [ $^4S$ ] + O [ $^3P$ ]

<u>Collision Energy (eV)</u>	<u>Scattering Cross-Section Matrix, <math>\sigma_{ij}</math></u>			
	$\sigma (a_0^{-2})$	$\sigma (cm^2)$		
0.3375	2.98 1.5-06	1.9-07 5.97	8.34-17 4.2-23	5.3-24 1.67-16
0.6096	1.10 3.7-06	7.6-08 5.97	3.08-17 1.0-22	2.1-24 1.67-16
0.8817	0.90 2.1-06	5.6-07 5.46	2.52-17 5.9-23	1.6-23 1.53-16
1.1538	1.96 8.9-07	2.9-07 5.24	5.49-17 2.5-23	8.1-24 1.47-16
1.4259	2.71 1.3-05	4.9-06 6.94	7.59-17 3.6-22	1.4-22 1.94-16
1.6980	2.59 3.4-06	1.4-06 6.31	7.25-17 9.5-23	3.9-23 1.77-16
1.9702	2.39 4.0-07	1.8-07 6.05	6.69-17 1.1-23	5.0-24 1.69-16

TABLE 6

MOLECULAR CORRELATION DIAGRAM FOR  
 $O^+ + N_2 \rightarrow NO^+ + N$

$O^+ [{}^4S_u] + N_2 [X {}^1\Sigma_g^+]$	$NO^+ [X {}^1\Sigma^+] + N [{}^4S_u]$
$E = 0.0 \text{ eV}$	$E = -1.09 \text{ eV}$
$O [{}^3P_g] + N_2^+ [X {}^2\Sigma_g^+]$	$NO^+ [X {}^1\Sigma^+] + N [{}^2D_u]$
$E = 1.94 \text{ eV}$	$E = 1.29 \text{ eV}$
$O [{}^3P_g] + N_2^+ [A {}^2\Pi_u]$	$NO^+ [X {}^1\Sigma^+] + N [{}^2P_u]$
$E = 3.05 \text{ eV}$	$E = 2.49 \text{ eV}$
$O^+ [{}^2D_u] + N_2 [X {}^1\Sigma_g^+]$	$NO [X {}^2\Pi] + N^+ [{}^3P_g]$
$E = 3.32 \text{ eV}$	$E = 4.17 \text{ eV}$
$O [{}^1D_g] + N_2^+ [X {}^2\Sigma_g^+]$	$NO^+ [a {}^3\Sigma^+] + N [{}^4S_u]$
$E = 3.91 \text{ eV}$	$E = 5.41 \text{ eV}$
$O^+ [{}^2P_u] + N_2 [X {}^1\Sigma_g^+]$	$NO [X {}^2\Pi] + N^+ [{}^1D_g]$
$E = 5.02 \text{ eV}$	$E = 6.07 \text{ eV}$
$O [{}^1D_g] + N_2^+ [A {}^2\Pi_u]$	$NO^+ [b {}^3\Pi] + N [{}^4S_u]$
$E = 5.03 \text{ eV}$	$E = 6.14 \text{ eV}$
$O [{}^3P_g] + N_2^+ [B {}^2\Sigma_u^+]$	$NO^+ [w {}^3\Delta] + N [{}^4S_u]$
$E = 5.11 \text{ eV}$	$E = 6.54 \text{ eV}$
$O [{}^1S_g] + N_2^+ [X {}^2\Sigma_g^+]$	$NO^+ [b' {}^3\Sigma^+] + N [{}^4S_u]$
$E = 6.13 \text{ eV}$	$E = 7.24 \text{ eV}$
$O^+ [{}^4S_u] + N_2 [A {}^3\Sigma_u^+]$	$NO^+ [A {}^1\Sigma^-] + N [{}^4S_u]$
$E = 6.16 \text{ eV}$	$E = 7.44 \text{ eV}$

DNA DISTRIBUTION LIST

Department of Defense

Director  
Defense Advanced Research Projects Agency  
1400 Wilson Boulevard  
Arlington, VA 22209

1 cy ATTN: TIO  
1 cy ATTN: STO  
1 cy ATTN: NRM0

Director  
Defense Communications Agency  
8th Street and Courthouse Road  
Arlington, VA 22204

3 cys ATTN: MECN Office

Defense Technical Information Center  
Cameron Station  
Alexandria, VA 22314

12 cys ATTN: TC

Director  
Defense Nuclear Agency  
Washington, DC 20305

1 cy ATTN: STTL  
1 cy ATTN: DDST  
3 cys ATTN: RAAE  
1 cy ATTN: RAEV  
2 cys ATTN: TITL

Joint Chiefs of Staff  
Department of Defense  
Washington, D. C. 20301

1 cy ATTN: J-6

DNA DISTRIBUTION LIST

Department of Defense (Cont'd)

Director  
National Security Agency  
Fort George G. Meade, MD 20755

2 cys ATTN: Technical Library

Under Secretary of Defense (Research and Engineering)  
Department of Defense  
Washington, D. C. 20301

2 cys ATTN: DDS&SS

Department of Commerce

U. S. Department of Commerce  
Office of Telecommunications  
Institute for Telecommunication Sciences  
National Telecommunications and Information Administration  
Boulder, CO 80303

2 cys ATTN. W. F. Utlaut

U.S. Department of Commerce  
National Bureau of Standards  
Washington, D. C. 20234

1 cy ATTN: M. Krauss

Department of the Army

Commander/Director  
Atmospheric Sciences Laboratory  
U. S. Army Electronics Command  
White Sands Missile Range, NM 88002

2 cys ATTN: DELAS-EO  
F. E. Niles  
M. Heaps

Director  
U. S. Army Ballistic Research Laboratories  
Aberdeen Proving Grounds, MD 21005

1 cy ATTN: George E. Keller

DNA DISTRIBUTION LIST

Department of the Army (Cont'd)

Commander

U. S. Army Foreign Sciences and Technology Center  
220 7th Street, N. E.  
Charlottesville, VA 22901

1 cy ATTN: Robert Jones

U.S. Army Research Office  
Durham, NC 27705

2 cys ATTN: R. Mace

Department of the Navy

Chief of Naval Operations  
Department of the Navy  
Washington, D. C. 20350

1 cy ATTN: NOP 985

1 cy ATTN: NOP 094H

Office of Naval Research  
Department of the Navy  
800 North Quincy Street  
Arlington, VA 22217

1 cy ATTN: Code 465, R. G. Joiner

1 cy ATTN: Code 427, H. Mullaney

Commander

Naval Electronic Systems Command  
Department of the Navy  
Washington, D. C. 20360

1 cy ATTN: PME-117

1 cy ATTN: PME-117T

1 cy ATTN: PME-117-21

1 cy ATTN: PME-117-21A

1 cy ATTN: PME-117-22

DNA DISTRIBUTION LIST

Department of the Navy (Cont'd)

Director  
Naval Ocean Systems Center  
Electromagnetic Propagation Division  
271 Catalina Boulevard  
San Diego, CA 92152

1 cy ATTN: Code 2200, W. F. Moler  
1 cy ATTN: Code 2200, Ilan Rothmuller  
1 cy ATTN: Code 2200, John Bickel

Naval Postgraduate School  
Monterey, CA 93940

1 cy ATTN: Code 0142  
1 cy ATTN: Code 1424

Office of Naval Research, Dept. of the Navy  
Arlington, VA 22217

1 cy ATTN: Code 421, B. R. Junker  
1 cy ATTN: Code 465, R. G. Joiner  
1 cy ATTN: Code 427, H. Mullaney

Director  
Naval Research Laboratory  
4555 Overlook Avenue, S. W.  
Washington, D. C. 20375

1 cy ATTN: Code 7700, Timothy P. Coffey  
1 cy ATTN: Code 7709, Wahab Ali  
2 cys ATTN: Code 7750, John Davis  
1 cy ATTN: Code 2627

Commander  
Naval Surface Weapons Center (White Oak)  
Silver Spring, MD 20910

1 cy ATTN: Technical Library

Office of Naval Research Branch Office  
1030 East Green Street  
Pasadena, CA 91106

1 cy

DNA DISTRIBUTION LIST

Department of the Air Force

Commander

Air Force Geophysical Laboratory, AFSC  
L. G. Hanscom Air Force Base, MA 01731

1 cy ATTN: LKD, W. Swider  
1 cy ATTN: LKB, K. Champion  
1 cy ATTN: PHG, F. R. Innes  
1 cy ATTN: OPR, R. A. Armstrong  
1 cy ATTN: OPR, H. Gardiner  
1 cy ATTN: LKO, R. E. Hoffman  
1 cy ATTN: OPR, A. T. Stair  
1 cy ATTN: PHI, J. R. Jasperse

Director

Air Force Technical Applications Center  
Patrick Air Force Base, FL 32920

1 cy ATTN: TD  
1 cy ATTN: HQ 1035th TCHOG/TFS

Commander AF Weapons Laboratory  
Kirtland AFB, Albuquerque, NM 87117

1 cy ATTN: H. O. Dogliani  
1 cy ATTN: J. I. Generosa  
1 cy ATTN: SUL

Department of Defense Contractors

General Electric Company  
TEMPO - Center for Advanced Studies  
816 State Street  
Santa Barbara, CA 93102

1 cy ATTN: T. L. Stephens  
1 cy ATTN: Warren S. Knapp  
1 cy ATTN: DASIAC

Lockheed Missiles and Space Company  
3251 Hanover Street  
Palo Alto, CA 94304

1 cy ATTN: J. B. Reagan  
1 cy ATTN: W. Imhof  
1 cy ATTN: Martin Walt

DNA DISTRIBUTION LIST

Department of Defense Contractors (Cont'd)

Mission Research Corporation  
735 State Street  
Santa Barbara, CA 93101

1 cy ATTN: M. Scheibe  
1 cy ATTN: D. Sowle

Pacific-Sierra Research Corporation  
1456 Cloverfield Boulevard  
Santa Monica, CA 90404

1 cy ATTN: E. C. Field

Pennsylvania State University  
Ionospheric Research Laboratory  
College of Engineering  
318 Electrical Engineering - East Wing  
University Park, PA 16802

1 cy ATTN: John S. Nisbet  
1 cy ATTN: Les Hale  
1 cy ATTN: A. J. Ferraro  
1 cy ATTN: H. S. Lee

R&D Associates  
4640 Admiralty Way  
Marina Del Rey, CA 90291

1 cy ATTN: R. Lelevier  
1 cy ATTN: F. Gilmore  
1 cy ATTN: R. Turco

The Rand Corporation  
1700 Main Street  
Santa Monica, CA 90406

1 cy ATTN: Cullen Crain

Professor Chalmers F. Sechrist  
155 Electrical Engineering Building  
University of Illinois  
Urbana, IL 61801

1 cy ATTN: C. Sechrist

DNA DISTRIBUTION LIST

Department of Defense Contractors (Cont'd)

SRI International  
333 Ravenswood Avenue  
Menlo Park, CA 94025

1 cy ATTN: Allen M. Peterson  
1 cy ATTN: Ray L. Leadabrand  
1 cy ATTN: J. R. Peterson  
1 cy ATTN: F. T. Smith

University of Pittsburgh  
Dept. of Physics and Astronomy  
Pittsburgh, PA 15260

1 cy ATTN: M. A. Biondi  
1 cy ATTN: F. Kaufman  
1 cy ATTN: W. Fite  
1 cy ATTN: J. N. Bardsley  
1 cy ATTN: E. Zipf

General Electric Co., Space Division, VFSC  
Goddard Blvd., King of Prussia  
P. O. Box 8555  
Philadelphia, PA 19101

1 cy ATTN: M. H. Bortner

National Oceanic & Atmospheric Admin.  
Environmental Research Laboratories  
Dept. of Commerce  
Boulder, CO 80302

1 cy ATTN: E. E. Ferguson  
1 cy ATTN: F. Fehsenfeld

Photometrics, Inc.  
4 Arrow Drive  
Woburn, MA 01801

1 cy ATTN: I. L. Kofsky

DNA DISTRIBUTION LIST

Department of Defense Contractors (Cont'd)

Harvard College Observatory  
Cambridge, MA 02138

1 cy ATTN: A. Dalgarno  
1 cy ATTN: D. E. Freeman

Utah State University  
Logan, UT 84322

1 cy ATTN: K. D. Baker

United Technologies Research Center  
East Hartford, CT 06108

1 cy ATTN: G. A. Peterson  
1 cy ATTN: H. H. Michels

Stewart Radiance Laboratories  
1 De Angelo Drive  
Bedford, MA 01730

1 cy ATTN: R. D. Sharma  
1 cy ATTN: J. C. Ulwick

Aerodyne Research, Inc.  
Crosby Drive  
Bedford, MA 01730

1 cy ATTN: M. Camac

Visidyne, Inc.  
NW Industrial Park  
Burlington, MA 01803

1 cy ATTN: T. C. Degges  
1 cy ATTN: C. H. Humphrey  
1 cy ATTN: H. J. R. Smith

Physical Sciences, Inc.  
Lakeside Office Park  
Wakefield, MA 01880

1 cy ATTN: G. Caledonia  
1 cy ATTN: T. Rawlins

DNA DISTRIBUTION LIST

Department of Defense Contractors (Cont'd)

Jet Propulsion Laboratory, CIT  
Pasadena, CA 91103

1 cy ATTN: S. Prasad

BC Space Data Analysis Laboratory  
885 Centre Street  
Newton, MA 02159

1 cy ATTN: S. Guberman

R&D Associates  
1401 Wilson Boulevard  
Arlington, VA 22209

1 cy ATTN: H. Mitchell

Lockheed  
Huntsville, AL 35803

1 cy ATTN: D. Divis

1 cy ATTN: C. M. Bowden

Spectral Sciences Inc.  
99 S. Bedford Street  
Burlington, MA, 01803

1 cy ATTN: F. Bien

**DATE  
ILME**